



HAL
open science

Mathematical analysis of a HIV model with quadratic logistic growth term

Xinyue Fan, Claude-Michel Brauner, Linda Wittkop

► **To cite this version:**

Xinyue Fan, Claude-Michel Brauner, Linda Wittkop. Mathematical analysis of a HIV model with quadratic logistic growth term. *Discrete and Continuous Dynamical Systems - Series B*, 2012, 17 (7), pp.27. 10.3934/dcdsb.2012.17.2359 . hal-00537467v2

HAL Id: hal-00537467

<https://hal.science/hal-00537467v2>

Submitted on 25 May 2012

HAL is a multi-disciplinary open access archive for the deposit and dissemination of scientific research documents, whether they are published or not. The documents may come from teaching and research institutions in France or abroad, or from public or private research centers.

L'archive ouverte pluridisciplinaire **HAL**, est destinée au dépôt et à la diffusion de documents scientifiques de niveau recherche, publiés ou non, émanant des établissements d'enseignement et de recherche français ou étrangers, des laboratoires publics ou privés.

MATHEMATICAL ANALYSIS OF A HIV MODEL WITH QUADRATIC LOGISTIC GROWTH TERM

XINYUE FAN †

School of Mathematical Sciences
Xiamen University, 361005 Xiamen, China

CLAUDE-MICHEL BRAUNER ‡

School of Mathematical Sciences
Xiamen University, 361005 Xiamen, China

and

Institut de Mathématiques de Bordeaux
Université de Bordeaux, 33405 Talence Cedex, France

LINDA WITTKOP

(M.D.) INSERM U897, Centre de recherche Epidémiologie et Biostatistique
ISPED, Université de Bordeaux, 33076 Bordeaux Cedex, France

and

Centre Hospitalier Universitaire de Bordeaux, 33076 Bordeaux Cedex, France

(Communicated by the associate editor name)

ABSTRACT. We consider a model of disease dynamics in the modeling of Human Immunodeficiency Virus (HIV). The system consists of three ODEs for the concentrations of the target T cells, the infected cells and the virus particles. There are two main parameters, N , the total number of virions produced by one infected cell, and r , the logistic parameter which controls the growth rate. The equilibria corresponding to the infected state are asymptotically stable in a region (\mathcal{I}), but unstable in a region (\mathcal{P}). In the unstable region, the levels of the various cell types and virus particles oscillate, rather than converging to steady values. Hopf bifurcations occurring at the interfaces are fully investigated via several techniques including asymptotic analysis. The Hopf points are connected through a “snake” of periodic orbits [24]. Numerical results are presented.

1. Introduction. CD4⁺ T lymphocytes (CD4⁺ cells) are the main target for the Human Immunodeficiency Virus (HIV) [9]. During acute infection an initial peak of HIV RNA (viral load) and a massive depletion in CD4⁺ cell count is observed and after 3-6 months of infection the viral load and CD4⁺ cell count reach a more stable level (steady state) [16]. Without antiretroviral treatment the asymptotic chronic state lasts for around 10 years [2] before an increase in viral load and an accelerated decrease in CD4⁺ cell count is observed. Ultimately, the progressive destruction of the immune system leads to the so-called Acquired Immunodeficiency Syndrome (AIDS) and death (see Fig. 1).

The immune response and the mechanisms for T-cell depletion during chronic infection are still not completely understood [25]. However, numerous mathematical models based on ordinary differential equations have been proposed to study the HIV-host interaction in primary HIV infection and helped to understand the HIV dynamics ([16, 29, 32] and

2000 *Mathematics Subject Classification.* Primary: 34A34; Secondary: 34D20, 92C50.

Key words and phrases. HIV modeling, stability, Hopf bifurcation, orbits, snakes.

† New affiliation: College of Science, Guizhou University, 550025 Guiyang, China.

‡ Corresponding author.

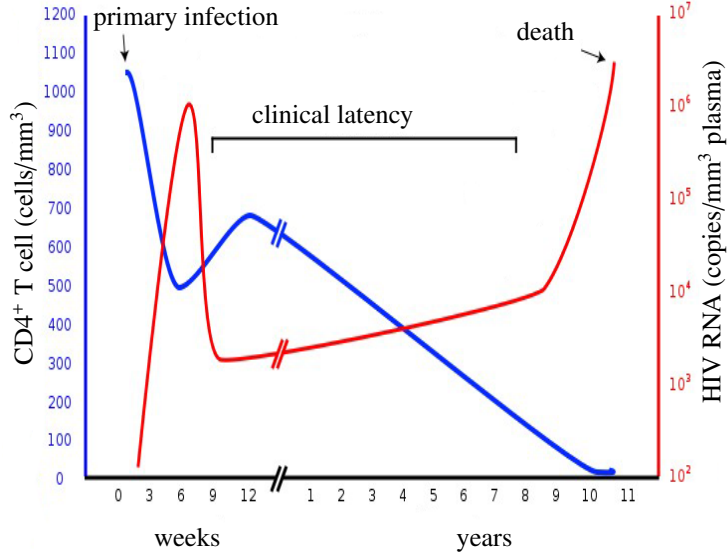


FIGURE 1. Typical course of HIV infection. Patterns of $CD4^+$ T-cell decline and virus load increase vary greatly from one patient to another, as do the actual values of viral RNA load. (Modified from Pantaleo et al. [27]).

[31] for a review). Further, mathematical models helped to gain biological insights of viral load and $CD4^+$ cell count evolution after treatment start [28, 29] and helped to understand the cellular viral reservoir, e.g. HIV infected memory $CD4^+$ cells whose half life was estimated to be 44 months [12, 19, 33]. Other cell types, e.g. monocytes or dendritic cells and anatomical sites, e.g. the central nervous system, may also constitute a reservoir for HIV (for a review, see [3]).

In this article we will study a basic model for HIV-host interaction (1)-(3) including three variables [31]. Let T denote the concentration of uninfected $CD4^+$ T cells, I the concentration of infected $CD4^+$ cells and V the concentration of free virus particles. For simplicity, we will call V the virus throughout the paper. The system reads:

$$\frac{dT}{dt} = \alpha - \mu_T T + rT \left(1 - \frac{T}{T_{max}}\right) - \gamma VT, \quad (1)$$

$$\frac{dI}{dt} = \gamma VT - \mu_I I, \quad (2)$$

$$\frac{dV}{dt} = N\mu_I I - \mu_V V. \quad (3)$$

This model is based on the hypotheses that uninfected $CD4^+$ T cells are produced from precursors in the thymus by a constant rate α and that they die by a constant rate μ_T . Free virus infects $CD4^+$ cells by a rate proportional to their abundance γVT and these infected $CD4^+$ cells will die at a rate μ_I . One infected $CD4^+$ cell will produce N free virions during its lifespan (3) and the term μ_V represents the clearance rate of the free virus. In healthy individuals the $CD4^+$ T-cell count is around 1000 cells/mm³ and by homeostatic processes the body tries to maintain the T-cell count [17, 18]. We introduce a quadratic logistic term

as previously proposed [30, 31] to consider the homeostatic process for the $CD4^+$ T-cell count. We thus assume that the uninfected $CD4^+$ cells proliferate logistically as it is very likely that the proliferation will shut off once the normal/maximal level of $CD4^+$ T-cell count is reached. The maximal $CD4^+$ T-cell proliferation rate r (see (1)) would be obtained by the absence of a population limit. T_{max} represents the normal/maximal density of $CD4^+$ T cells at which $CD4^+$ T-cell proliferation shuts off. Mathematically it will play the role of a large perturbation parameter. We refer to Table 1 for a gamut of numerical data (see, e.g., [30][4]). Typical evolution profiles are shown in Fig. 2.

TABLE 1. Variables and Parameters

Parameters and variables		Values
Dependent variables		
T	Uninfected $CD4^+$ T-cell population	mm^{-3}
I	Infected $CD4^+$ T-cell density	mm^{-3}
V	HIV population size	mm^{-3}
Parameters and constants		
r	Proliferation rate of the $CD4^+$ T-cell population	0.2 day^{-1}
N	Number of virus produced by infected cells	1000
α	Production rate for uninfected $CD4^+$ T cells	$1.5 \text{ day}^{-1} mm^{-3}$
γ	Infection rate of uninfected $CD4^+$ T cells	$0.001 \text{ mm}^3 \text{ day}^{-1}$
T_{max}	Maximal population level of $CD4^+$ T cells at which the $CD4^+$ T-cell proliferation shuts off	1500 mm^{-3}
μ_T	Death rate of uninfected $CD4^+$ T-cell population	0.1 day^{-1}
μ_I	Death rate of infected $CD4^+$ T-cell population	0.5 day^{-1}
μ_V	Clearance rate of free virus	10 day^{-1}
Derived variables		
T_0	$CD4^+$ T-cell population for HIV negative persons	mm^{-3}

In the absence of virus, the T-cell population has a steady state value:

$$T_0 = \frac{(r - \mu_T) + \sqrt{(r - \mu_T)^2 + \frac{4r\alpha}{T_{max}}}}{2r} T_{max}.$$

Note that the quantity $r - \mu_T$, the net T-cell proliferation rate, needs not to be positive (see [30, p. 86]).

We set $X(t) = (T(t), I(t), V(t))$ and write the system (1)-(3) as the smooth Cauchy problem:

$$\frac{dX}{dt}(t) = \mathcal{F}(X(t)), \quad X(0) = X_0, \quad (4)$$

where X_0 corresponds to non-negative initial conditions (see App. B).

It is easily seen that the system (4) has two possible nonnegative equilibria:

(i) the uninfected steady state $X_u = (T_u, I_u, V_u)$:

$$T_u = T_0 = \frac{(r - \mu_T) + \sqrt{(r - \mu_T)^2 + \frac{4r\alpha}{T_{max}}}}{2r} T_{max}, \quad I_u = 0, \quad V_u = 0, \quad (5)$$

which corresponds to a positive equilibrium in case of no infection;

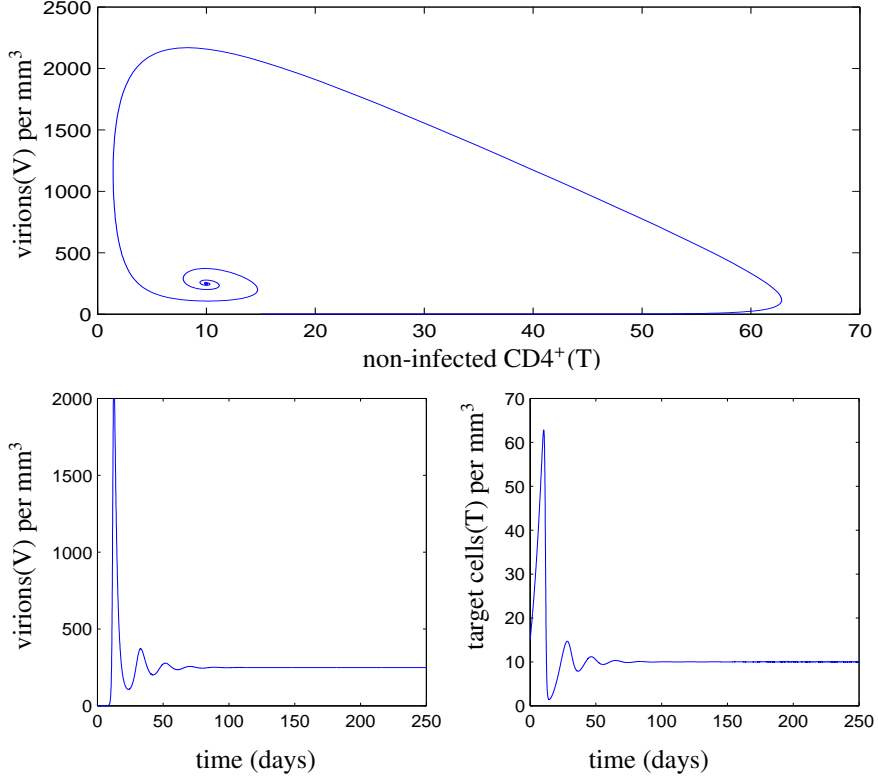


FIGURE 2. Typical profiles of virus vs. target cells in the phase plane (front), virus (left) and target cells (right) in the case of stable infection. Here $N = 1000$, $r = 0.2$. The other quantities are as in Table 1.

(ii) the infected steady state $X_i = (T_i, I_i, V_i)$:

$$\begin{aligned} T_i &= \frac{\mu_V}{\gamma N}, & I_i &= \frac{\alpha}{\mu_I} - \frac{\mu_T \mu_V}{N \gamma \mu_I} + \frac{r \mu_V}{N \gamma \mu_I} \left(1 - \frac{\mu_V}{N \gamma T_{max}}\right), \\ V_i &= \frac{\alpha N}{\mu_V} - \frac{\mu_T}{\gamma} + \frac{r}{\gamma} \left(1 - \frac{\mu_V}{N \gamma T_{max}}\right). \end{aligned} \quad (6)$$

The infected steady state or “seropositivity steady state” corresponds to a positive equilibrium in case of infection.

The basic reproduction number R_0 for the above described model reads:

$$R_0 = \frac{\gamma N T_0}{\mu_V}. \quad (7)$$

It denotes the average number of infected T cells derived from one infected T cell and is based on the definition of R_0 by epidemiologists [8]. As it can easily be seen, R_0 depends on the logistic parameter r , whereas its critical value is equal to unity for all r . R_0 was often considered as a bifurcation parameter to study stability properties of the two above described equilibria [6, 26]. De Leenheer and Smith [6] found sustained oscillations and that the steady state may be unstable when considering a system as described by (1)-(3) for $R_0 > 1$. Perelson, Kirschner and De Boer also observed sustained oscillations in a

model including a compartment of latently infected T cells [30]. However, their biological meaning remains unclear thus far.

Perelson et al. found that N , the number of free virions produced by one actively infected $CD4^+$ cell during its lifespan, needs to be above some critical level for successful HIV infection [30]. Therefore, in Section 2, we consider N and r as two independent parameters to study the properties of the “uninfected” and “infected” steady states. Simultaneously, T_{max} will play the role of a large perturbation parameter.

First, we determine two domains in the parameter space, respectively (\mathcal{U}) referring to “uninfected” ($R_0 < 1$) and (\mathcal{I}) referring to “infected” ($R_0 > 1$), see Fig. 3. The uninfected equilibrium is asymptotically stable in (\mathcal{U}) and unstable in (\mathcal{I}). For determining these two domains we use the classical Routh-Hurwitz criterion. This criterion ensures that the eigenvalues of the Jacobian matrix have negative real part if and only if the corresponding Hurwitz determinants D_j , $j = 1, 2, 3$, are positive. Note that the positive infected equilibrium exists in (\mathcal{I}) only.

Second, there is an unbounded subdomain (\mathcal{P}) in (\mathcal{I}), the symbol (\mathcal{P}) referring to “perturbation” (see below). In this subdomain (\mathcal{P}): (i) the positive infected equilibrium becomes unstable whereas it is asymptotically stable in the rest of (\mathcal{I}), and (ii) there are asymptotically stable periodic orbits with asymptotic phase. The boundary of (\mathcal{P}) is precisely the locus of points (N, r) such that $D_2 = 0$, explicitly parameterized by the mappings $r_1(N)$ and $r_2(N)$. When the logistic term $rT(1 - T/T_{max})$ is replaced by $rT(1 - (T + I)/T_{max})$, numerical evidence shows that (\mathcal{P}) is bounded (see App. A).

The subdomain (\mathcal{P}) may be biologically interpreted as a perturbation of the infection by a specific or unspecific immune response against HIV. An infection with other pathogens could lead to a non-specific immune response against HIV or existing specific memory T cells could be stimulated by cross-reactive stimulation [1]. Further, interventions to boost the immune response such as Interleukin-7 or Interleukin-2 treatment could lead to containment of HIV infection [22, 23].

Starting from Section 3, we fix N and take r as bifurcation parameter, which is logic as it is one of the crucial parameters in the host-pathogen interaction. We prove via a linear analysis that the infected equilibria X_i is unstable in the interior of the region (\mathcal{P}) and Hopf bifurcations occur on the boundary, namely at the points r_1 and r_2 .

The nonlinear analysis is fully developed in Section 4, which constitutes the core of the paper. We follow [15, 21] to compute the first Lyapunov coefficient and determine the direction and stability of the bifurcated branch of periodic orbits at the Hopf points $(X_i(r_1), r_1)$ and $(X_i(r_2), r_2)$. However, a relevant analysis is based on an asymptotic approach when T_{max} is large, especially the observation that the system (1)-(3) has a limit when $T_{max} \rightarrow +\infty$, in which a new bifurcation parameter is the net T-cell proliferation rate. In other words, the perturbation by the small parameter $1/T_{max}$ is regular at r_1 and we take advantage of it.

The last issue we address is the existence of a “bridge” between the family of periodic orbits at the two Hopf points $(X_i(r_1), r_1)$ and $(X_i(r_2), r_2)$. We are able to prove the existence of a “snake”, a maximal path of orbits, thanks to the theory of Mallet-Paret and Yorke [24].

Finally, we illustrate the results of this paper with a series of numerical computations.

2. Stability.

2.1. **Equilibria.** The notations are those of Section 1. More precisely, we state:

- (i) $N > 0$ and $r \geq 0$ are parameters;
- (ii) the quantities (with associated dimension) $\mu_T, \mu_I, \mu_V, \alpha$ and γ are fixed positive numbers throughout the paper;

(iii) T_{max} is a large perturbation parameter, larger than any finite combination of $\mu_T, \mu_I, \mu_V, \alpha$ and γ of the same dimension (mm^{-3}). In other words, we will make the hypothesis that

$$T_{max} \geq T_{max}^0(\mu_T, \mu_I, \mu_V, \alpha, \gamma), \quad (8)$$

where T_{max}^0 is fixed and large, and depends only of $\mu_T, \mu_I, \mu_V, \alpha$ and γ . In particular, this hypothesis contains the condition $T_{max} > \alpha/\mu_T$ of [30, p. 85].

We consider the possible nonnegative equilibria of the system (1)-(3) given by the formulas (5) and (6). At fixed $r \geq 0$, it is not difficult to compute the critical value at which $V_u = V_i = 0$:

$$N_{crit}(r) = \frac{\mu_V \left(-(r - \mu_T) + \sqrt{(r - \mu_T)^2 + \frac{4\alpha r}{T_{max}}} \right)}{2\alpha\gamma} = \frac{\mu_V}{\gamma T_0}. \quad (9)$$

Obviously, $N = N_{crit}(r)$ is equivalent to $R_0(N, r) = 1$, where (see (7)):

$$R_0(N, r) = \frac{\gamma N T_0(r)}{\mu_V}. \quad (10)$$

At $r = 0$, $N_{crit}(0) = \frac{\mu_T \mu_V}{\alpha\gamma}$, and, as $r \rightarrow +\infty$,

$$N_{crit}(r) \rightarrow N_{crit}(+\infty) = \frac{\mu_V}{\gamma T_{max}}.$$

It will follow from the proof of next theorem that the roles of parameters N and r can be inverted. A more convenient critical value is then defined by:

$$r_{crit}(N) = \frac{(\mu_T \mu_V - \gamma \alpha N)^+}{\mu_V \left(1 - \frac{\mu_V}{N \gamma T_{max}} \right)}, \quad N > N_{crit}(+\infty) = \frac{\mu_V}{\gamma T_{max}}. \quad (11)$$

Theorem 2.1. *We assume (8). In the first quarter plane of the (N, r) parameter space, there are two regions, (\mathcal{U}) for uninfected ($R_0(N, r) < 1$), and (\mathcal{I}) for infected ($R_0(N, r) > 1$) such that:*

(i) *in (\mathcal{U}) , the uninfected steady state $X_u = (T_u, I_u, V_u)$ is the only nonnegative equilibrium. In (\mathcal{I}) , there are two nonnegative equilibria, respectively X_u and the infected steady state $X_i = (T_i, I_i, V_i)$;*

(ii) *it holds $0 < T_u < T_{max}$ and, in (\mathcal{I}) , $0 < T_i < T_{max}$;*

(iii) *in (\mathcal{U}) , the uninfected steady state is asymptotically stable, in (\mathcal{I}) , the uninfected steady state is unstable.*

Proof. (i) It is an exercise to see that the mapping $r \mapsto N_{crit}(r)$ is decreasing and convex for $r > 0$, since $N_{crit}''(r) > 0$, $N_{crit}'(0) < 0$, and $N_{crit}'(r) \rightarrow 0$ as $r \rightarrow +\infty$. Therefore we can split the quarter plane $N > 0, r \geq 0$ in two domains, first (\mathcal{I}) which lies strictly above the graph of mapping $r \mapsto N_{crit}(r)$, second (\mathcal{U}) which lies below the graph.

(ii) Thanks to (8), on the one hand

$$\begin{aligned} T_u &= \frac{(r - \mu_T) + \sqrt{(r - \mu_T)^2 + \frac{4r\alpha}{T_{max}}}}{2r} T_{max} \\ &< \frac{(r - \mu_T) + \sqrt{(r - \mu_T)^2 + 4\mu_T r}}{2r} T_{max} = T_{max}. \end{aligned}$$

On the other hand, $T_i = \mu_V/(\gamma N) < T_{max}$ whenever $N > N_{crit}(r) = \mu_V/(\gamma T_{max})$.

(iii) The study of the stability of the uninfected solution is easy, however we include it for

the convenience of the reader. Let $r \geq 0$ be fixed. We compute explicitly the eigenvalues of the Jacobian matrix

$$J(X_u) = \begin{pmatrix} r - \mu_T - \frac{2rT_u}{T_{max}} & 0 & -\gamma T_u \\ 0 & -\mu_I & \gamma T_u \\ 0 & N\mu_I & -\mu_V \end{pmatrix}.$$

They are all real:

$$\begin{aligned} \lambda_1 &= -\sqrt{(-r + \mu_T)^2 + 4\frac{r\alpha}{T_{max}}} < 0, \\ \lambda_2 &= -\frac{1}{2}\left((\mu_I + \mu_V) + \sqrt{(\mu_I + \mu_V)^2 - 4(\mu_I\mu_V - N\gamma\mu_I T_u)}\right) < 0, \\ \lambda_3 &= \frac{1}{2}\left(-(\mu_I + \mu_V) + \sqrt{(\mu_I + \mu_V)^2 - 4\mu_I\mu_V\left(1 - \frac{N}{N_{crit}(r)}\right)}\right). \end{aligned}$$

It is clear that $\lambda_3 < 0$ for $N < N_{crit}(r)$, therefore the three eigenvalues are negative. As long there is no eigenvalue on the imaginary axis, it is well-known that linear stability yields nonlinear stability for a smooth system of the form (4), since, by the Hartman-Grobman theorem (see, e.g. [14, IX]), near a hyperbolic equilibrium the system is locally topologically equivalent to its linearization. \square

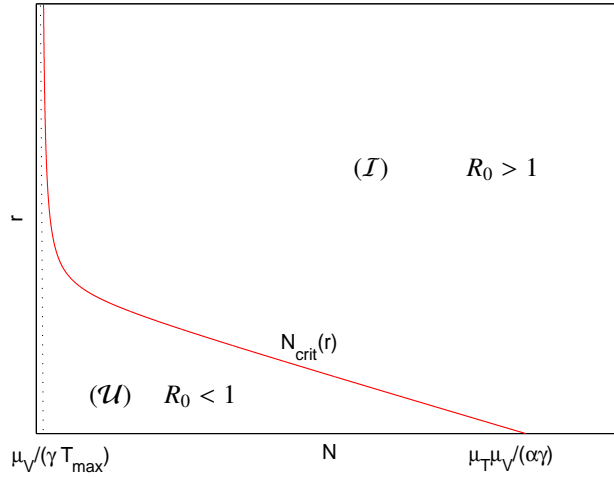


FIGURE 3. Profile of the curve $r \mapsto N_{crit}(r)$ (i.e. $R_0 = 1$) which defines the two domains (\mathcal{U}) and (\mathcal{I}) . With the values of Table 1, N_{crit} decreases from $\mu_T\mu_V/\alpha\gamma = 666.67$ to $\mu_V/\gamma T_{max} = 6.67$. See (11) for the reverse mapping $N \mapsto r_{crit}(N)$.

The issue of the stability of the infected solution is obviously more complicated. For $(N, r) \in (\mathcal{I})$, we consider the Jacobian matrix:

$$J(X_i) = \begin{pmatrix} r - \mu_T - \frac{2rT_i}{T_{max}} - \gamma V_i & 0 & -\gamma T_i \\ \gamma V_i & -\mu_I & \gamma T_i \\ 0 & N\mu_I & -\mu_V \end{pmatrix}. \quad (12)$$

The spectrum of $J(X_i)$ is given by the roots (three real roots or one real and two complex conjugates) of the following characteristic equation:

$$\lambda^3 + d_1\lambda^2 + d_2\lambda + d_3 = 0, \quad (13)$$

where the coefficients (functions of N and r) read:

$$\begin{aligned} d_1 &= \mu_I + \mu_V + \frac{\gamma\alpha N}{\mu_V} + \frac{r\mu_V}{\gamma T_{max}N}, \\ d_2 &= \frac{\gamma N\alpha\mu_I}{\mu_V} + \gamma\alpha N + \frac{r\mu_I\mu_V}{\gamma T_{max}N} + \frac{r\mu_V^2}{\gamma T_{max}N}, \\ d_3 &= \left(\mu_I\mu_V - \frac{\mu_V^2\mu_I}{\gamma T_{max}N} \right) r + \gamma N\alpha\mu_I - \mu_V\mu_I\mu_T. \end{aligned} \quad (14)$$

2.2. Study of the characteristic equation (13). We recall that the Routh-Hurwitz criterion gives necessary and sufficient conditions for all the roots of a real polynomial to have negative real parts (see, e.g., [13, Chap. XV]). Therefore it provides a stability analysis only by examining the coefficients of the characteristic polynomial, without computing the eigenvalues. In the case of (13), the roots have negative real part if and only if the corresponding Hurwitz determinants are positive:

$$D_1 = d_1 > 0, \quad D_2 = d_1d_2 - d_3 > 0, \quad D_3 = d_3D_2 > 0.$$

In other words, the roots of (13) have negative real part if and only if

$$d_1 > 0, \quad d_3 > 0, \quad D_2 = d_1d_2 - d_3 > 0. \quad (15)$$

Obviously, $d_1 > 0$. We compute $d_3 = 0$, which is equivalent to

$$\alpha\gamma N^2 + (r\mu_V - \mu_V\mu_T)N - \frac{r\mu_V^2}{\gamma T_{max}} = 0,$$

whose positive solution is $N_{crit}(r)$. Therefore $d_3 > 0$ for $N > N_{crit}(r)$, i.e., whenever $(N, r) \in (\mathcal{I})$.

Next, we compute the leading Hurwitz determinant

$$D_2 = d_1d_2 - d_3 = \frac{1}{\mu_V^2(T_{max})^2\gamma^2N^2}(Ar^2 + Br + C) \quad (16)$$

as a function of the parameters N and r . The coefficients read:

$$\begin{aligned} A &= \mu_V^5 + \mu_V^4\mu_I, \\ B &= -N\gamma T_{max}\mu_V^2(N\gamma\mu_I\mu_V T_{max} - 2\gamma\alpha N\mu_V - 2N\gamma\mu_I\alpha \\ &\quad - \mu_V^3 - 3\mu_V^2\mu_I - \mu_I^2\mu_V), \\ C &= N^2\gamma^2(T_{max})^2(N\gamma\mu_V^3\alpha + N\gamma\mu_I\alpha\mu_V^2 + N\gamma\mu_I^2\mu_V\alpha + \gamma^2N^2\alpha^2\mu_V \\ &\quad + \gamma^2N^2\alpha^2\mu_I + \mu_V^3\mu_I\mu_T). \end{aligned}$$

The issue is to determine the subdomains of (\mathcal{I}) where $D_2(N, r)$ is respectively positive and negative and, as far as possible, the locus of points where $D_2(N, r) = 0$.

Obviously, D_2 has the sign of $Ar^2 + Br + C$. Note that $A > 0$ is fixed, only B and C depend on N . Whereas $C > 0$, $B(N)$ vanishes at

$$N_0 = \frac{\mu_V(3\mu_I\mu_V + \mu_I^2 + \mu_V^2)}{\gamma(\mu_I\mu_V T_{max} - 2\mu_V\alpha - 2\mu_I\alpha)}. \quad (17)$$

Since T_{max} is large with respect to the other quantities, N_0 is positive but small:

$$N_{crit}(+\infty) = \frac{\mu_V}{\gamma T_{max}} < N_0 < N_{crit}(0).$$

Therefore, for $N_{crit}(+\infty) \leq N < N_0$, we have $B > 0$, and $B < 0$ for $N > N_0$.

To determine the sign of the polynomial $Ar^2 + Br + C$, we compute the discriminant

$$\Delta(N) = B^2 - 4AC = N^2 \gamma^2 (T_{max})^2 \mu_V^5 (aN^2 + bN + c),$$

which in turn is of the sign of $aN^2 + bN + c$.

The coefficients a, b and c read:

$$\begin{aligned} a &= \gamma^2 T_{max} \mu_I (-4\mu_I \alpha + \mu_I T_{max} \mu_V - 4\mu_V \alpha), \\ b &= -2\gamma \mu_I \mu_V (T_{max} \mu_I^2 + 3\mu_I T_{max} \mu_V - 4\mu_I \alpha + \mu_V^2 T_{max} - 4\mu_V \alpha), \\ c &= \mu_V (\mu_V^4 + 6\mu_V^3 \mu_I + 11\mu_V^2 \mu_I^2 - 4\mu_V^2 \mu_I \mu_T + 6\mu_V \mu_I^3 - 4\mu_I^2 \mu_V \mu_T + \mu_I^4). \end{aligned}$$

For T_{max} large enough, $a > 0$ and $b < 0$. However, the sign of c , which does not contain T_{max} , depends on the other quantities. Next we compute:

$$\begin{aligned} \delta &= b^2 - 4ac \\ &= 16\gamma^2 \mu_I (\mu_I + \mu_V) \mu_V (T_{max} \alpha \mu_I^4 + 4T_{max} \alpha \mu_V \mu_I^3 + 5\mu_I^2 \mu_V^2 T_{max} \alpha \\ &\quad + \mu_I^2 \mu_V^2 (T_{max})^2 \mu_T + 4\mu_I^2 \mu_V \alpha^2 - 4\mu_I^2 \mu_V T_{max} \alpha \mu_T + 4\mu_I \mu_V^3 T_{max} \alpha \\ &\quad + 4\mu_I \mu_V^2 \alpha^2 - 4\mu_I T_{max} \alpha \mu_V^2 \mu_T + \mu_V^4 \alpha T_{max}). \end{aligned}$$

For large T_{max} , δ has the sign of the coefficient of $(T_{max})^2$, hence $\delta > 0$.

The roots of $\Delta = 0$, namely those of $aN^2 + bN + c = 0$, are $N_1 < N_2$:

$$N_1 = \frac{-b - \sqrt{\delta}}{2a}, \quad N_2 = \frac{-b + \sqrt{\delta}}{2a}. \quad (18)$$

It is clear that $N_2 > 0$, while N_1 has the sign of c . However, N_1 plays a role only if larger than $N_{crit}(+\infty)$. We also remark that N_2 is small for large T_{max} , therefore $N_2 < N_{crit}(0)$.

It is easy to determine the position of N_0 , see (17), with respect to N_1 and N_2 . Actually, since $B(N_0) = 0$, $\Delta(N_0) = -4AC < 0$, hence $aN_0^2 + bN_0 + c < 0$. Therefore it holds:

Lemma 2.2. $N_1 < N_0 < N_2 < N_{crit}(0)$.

Now we are in position to begin our discussion following the position of N .

Case 1. It corresponds to $N_1 < N < N_2$. In such a case, $aN^2 + bN + c < 0$, hence $\Delta(N) < 0$. Obviously, $Ar^2 + Br + C$ has the sign of A which is positive.

Case 2. It corresponds to $N < N_1$ or $N > N_2$.

(i) If $N < N_1$, then, by Lemma 2.2, $B > 0$. Hence, $Ar^2 + Br + C > 0$ for any $r \geq 0$ since $A, B, C > 0$. It thus follows that $D_2 > 0$.

(ii) If $N > N_2$, then, by Lemma 2.2, $B < 0$. Since $\Delta > 0$, the equation $Ar^2 + Br + C = 0$ admits the two real and positive roots

$$r_1(N) = \frac{-B - \sqrt{\Delta}}{2A}, \quad r_2(N) = \frac{-B + \sqrt{\Delta}}{2A}. \quad (19)$$

Consequently, the Hurwitz determinant D_2 is positive for $r_{crit}(N) \leq r < r_1(N)$ and $r > r_2(N)$, it vanishes at $r = r_1(N)$ and $r = r_2(N)$, it is negative for $r_1(N) < r < r_2(N)$.

Case 3. It corresponds to $N = N_1$ or $N = N_2$. In such a case, $\Delta = 0$ and the polynomial $Ar^2 + Br + C$ has the double root $r = -B/2A$. However, this solution makes sense only if $B < 0$, namely $N > N_0$. Then by Lemma 2.2, we discard the case $N = N_1$. Therefore at $N = N_2$, D_2 is positive except at $r(N_2) = -B/2A$ where it vanishes.

Remark 1. It is important to see that $r_{crit}(N) < r_1(N)$ whenever $N \geq N_2$. For $N_2 \leq N \leq N_{crit}(0)$, if $r_{crit}(N) = r_1(N)$, then d_3 and D_2 vanish simultaneously which is impossible. When $N > N_{crit}(0)$, $r_{crit}(N) = 0$ and $r_1(N) > 0$.

We are now in position to define the subdomain (\mathcal{P}) of (\mathcal{I}) by

$$(\mathcal{P}) = \{(N, r), N \geq N_2, r_1(N) \leq r \leq r_2(N)\}, \quad (20)$$

with

$$N_2 = \frac{-b + \sqrt{\delta}}{2a}, \quad r_1(N) = \frac{-B - \sqrt{\Delta}}{2A}, \quad r_2(N) = \frac{-B + \sqrt{\Delta}}{2A},$$

and at $N = N_2$, the endpoint of (\mathcal{P}) , $r_1 = r_2 = -B/2A$.

Theorem 2.3. Under the hypothesis (8), the infected equilibrium $X_i = (T_i, I_i, V_i)$ is asymptotically stable for $(N, r) \in (\mathcal{I} \setminus \mathcal{P})$.

Proof. Under the hypothesis (8), the leading Hurwitz determinant $D_2(N, r)$ is respectively negative in the interior of the subdomain (\mathcal{P}) of (\mathcal{I}) , positive in $(\mathcal{I} \setminus \mathcal{P})$, and it vanishes on the boundary of (\mathcal{P}) . Then, the theorem follows from the Ruth-Hurwitz criterion. \square

However, we can not infer from Theorem 2.3 that the infected equilibrium X_i is unstable in (\mathcal{P}) or in its interior. This issue will be addressed in Section 3.

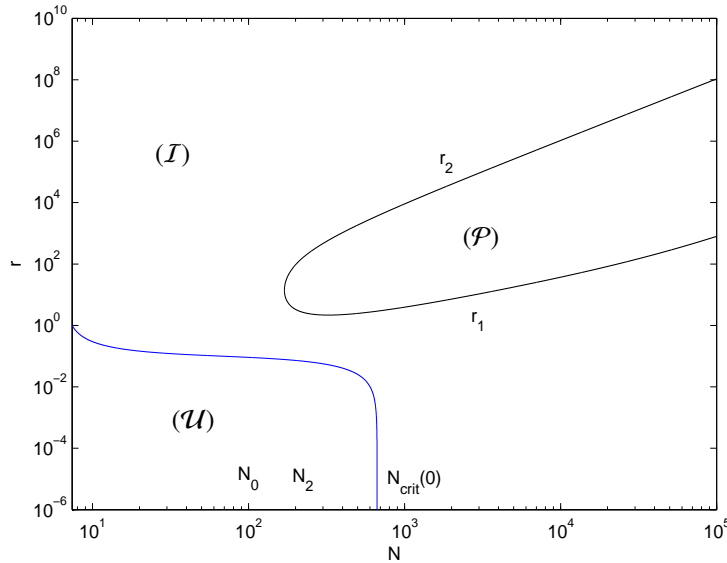


FIGURE 4. Full portrait of the domains (\mathcal{I}) , (\mathcal{U}) and (\mathcal{P}) in the (N, r) parameter space, in logarithmic scales. Numerical values are as in Table 1. Here $N_0 = 154.35$, $N_2 = 169.81$, $N_{crit}(0) = 666.67$, $r_{crit}(N_2) = 0.08$, $r_1(N_2) = r_2(N_2) = 14.03$.

3. Hopf bifurcation and instability. From now on, we take the logistic parameter r as a bifurcation parameter, whereas $N > 0$ is fixed. In Subsection 2.2, we already used the fact that N_2 , the endpoint of the subdomain (\mathcal{P}) , is small for large T_{max} . More precisely, it is easy to see from (18) that

$$N_2 = \frac{\mu_I^2 + 3\mu_I\mu_V + \mu_V^2 + 2\sqrt{\mu_I\mu_V\mu_T(\mu_I + \mu_V)}}{\gamma\mu_I} \frac{1}{T_{max}} + o\left(\frac{1}{T_{max}}\right).$$

We assume hereafter that

$$T_{max} \geq T_{max}^1(\mu_T, \mu_I, \mu_V, \alpha, \gamma, N), \quad (21)$$

where $T_{max}^1(\mu_T, \mu_I, \mu_V, \alpha, \gamma, N) \geq T_{max}^0(\mu_T, \mu_I, \mu_V, \alpha, \gamma)$ (see (8)) is chosen large enough such that $0 < N_2 < N$.

3.1. Parametrization by the logistic parameter. Since $N > N_2$ it is clear that the vertical line through the point $(N, 0)$ intersects the subdomain (\mathcal{P}) . We consider the family of infected equilibria $X_i(r)$, smoothly parameterized by the logistic parameter $r \geq r_{crit} = r_{crit}(N)$. The other critical values of r are $r_1(N)$ and $r_2(N)$. Below we simply denote them by r_1 and r_2 .

We rewrite the system (4) as

$$\frac{dX}{dt}(t) = \mathcal{F}(X(t), r), \quad (22)$$

where \mathcal{F} is obviously a smooth function. In summary, the bifurcation parameter is $r \in (r_{crit}, +\infty)$, the equilibria are $X_i(r)$, and the two critical values of the bifurcation parameter are r_1 and r_2 .

The Jacobian matrix (12) reads

$$J(X_i(r)) = \begin{pmatrix} r - \mu_T - \frac{2rT_i}{T_{max}} - \gamma V_i(r) & 0 & -\gamma T_i \\ \gamma V_i(r) & -\mu_I & \gamma T_i \\ 0 & N\mu_I & -\mu_V \end{pmatrix}, \quad (23)$$

where

$$V_i(r) = \frac{\alpha N}{\mu_V} - \frac{\mu_T}{\gamma} + \frac{r}{\gamma} \left(1 - \frac{\mu_V}{N\gamma T_{max}}\right),$$

and the associated characteristic equation (13) is

$$\lambda^3 + d_1(r)\lambda^2 + d_2(r)\lambda + d_3(r) = 0, \quad (24)$$

see (14) for the expressions of the coefficients. We recall that $d_3 > 0$ in (I) , hence $d_3(r) > 0$ for $r > r_{crit}$. Let us denote by $\lambda_i(r)$, $i = 1, 2, 3$, the three eigenvalues. The mappings $r \mapsto \lambda_i(r)$ are continuous, and smooth except at exceptional points where two of the λ_i 's coincide as in Figure 5 (see [20, Chap. II]). At fixed r , one of the eigenvalues is real while the others are either real or complex conjugate. Since $d_1 > 0$, $d_2 > 0$ and $d_3 > 0$ in (I) , we immediately observe:

Lemma 3.1. *The polynomial (24) has no non-negative real root. At least one of the eigenvalues is negative whenever $r > r_{crit}$.*

We also have the notations, according to Subsection 13:

$$D_1(r) = d_1(r), \quad D_2(r) = d_1(r)d_2(r) - d_3(r). \quad (25)$$

The relation between the Hurwitz determinant $D_2(r)$ and the sums of pairs of λ_i 's is given by Orlando's formula (see, e.g., [13, Chap. XV]):

$$D_2(r) = -(\lambda_1(r) + \lambda_2(r))(\lambda_2(r) + \lambda_3(r))(\lambda_1(r) + \lambda_3(r)). \quad (26)$$

From the results of Section 2 and Theorem 2.3, we know that the infected equilibrium $X_f(r)$ is asymptotically stable whenever $r_{crit} < r < r_1$ or $r > r_2$. Stability may be lost when either $d_3(r) = 0$ or $D_2(r) = 0$. The former case corresponds to $r = r_{crit}$ where, say, $\lambda_3 = 0$ and

$$\lambda_{1,2} = \frac{1}{2} \left(-d_1 \pm \sqrt{d_1^2 - 4d_2} \right),$$

(see Figure 5). The latter case occurs at $r = r_1$ where a pair of purely imaginary complex roots exists, as we are going to see in the next subsection. As a consequence of Lemma 3.1, only a pair of complex conjugate eigenvalues may cross the imaginary axis, which leads to a Hopf bifurcation. Increasing r , stability is regained when $r > r_2$.

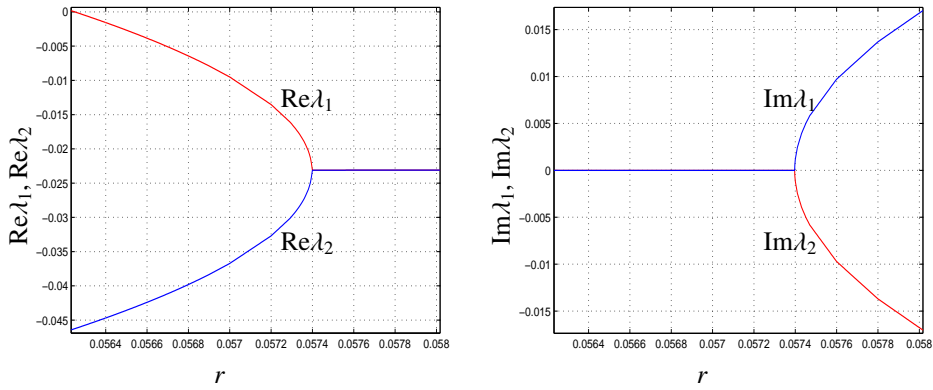


FIGURE 5. Real part (left) and imaginary part (right) of eigenvalues λ_1 and λ_2 as functions of the bifurcation parameter r at $N = 300$ (to fix ideas). The graphic starts at $r_{crit} = 0.05625$, $\lambda_1 = \lambda_2$ at $r = 0.05734$. The real eigenvalue $\lambda_3 < -10$ is not pictured.

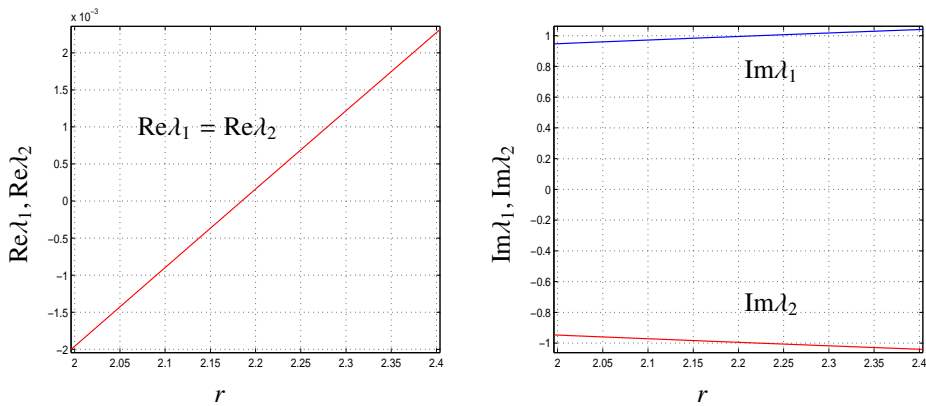


FIGURE 6. Real part (left) and imaginary part (right) of eigenvalues λ_1 and λ_2 as functions of the bifurcation parameter r at fixed $N = 300$. They cross the imaginary axis at $r_1 = 2.1846$.

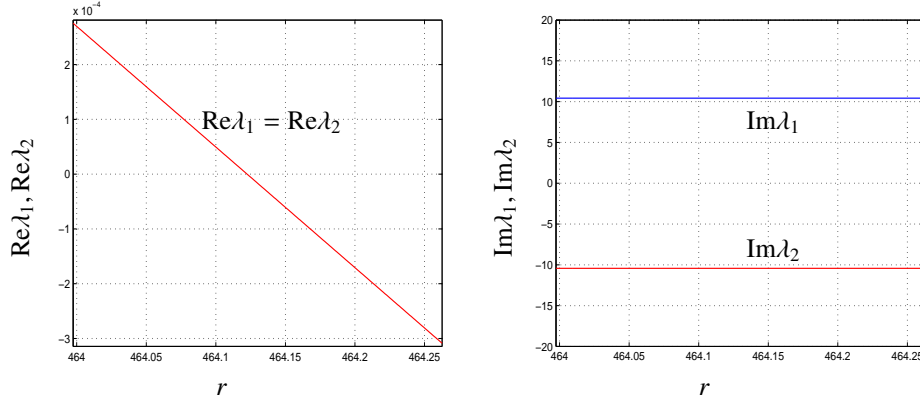


FIGURE 7. For larger r , real part (left) and imaginary part (right) of eigenvalues λ_1 and λ_2 as functions of the bifurcation parameter r at fixed $N = 300$. They cross the imaginary axis at $r_2 = 464.1225$.

3.2. Existence of two Hopf bifurcations. We are going to examine the critical values $r = r_1$ and $r = r_2$ and prove that they correspond to Hopf points. A detailed study of the Hopf bifurcations will be the subject of Section 4.

Lemma 3.2. (i) At $r = r_k$, $k = 1, 2$, the eigenvalues $\lambda_1(r_k)$ and $\lambda_2(r_k)$ are purely imaginary and conjugate:

$$\lambda_1(r_k) = i\omega_k, \quad \lambda_2(r_k) = -i\omega_k,$$

$$\omega_k = \sqrt{d_2(r_k)} = \sqrt{\frac{\gamma N \alpha \mu_I}{\mu_V} + \gamma \alpha N + \frac{r_k \mu_I \mu_V}{\gamma T_{max} N} + \frac{r_k \mu_V^2}{\gamma T_{max} N}}; \quad (27)$$

(ii) the third eigenvalue $\lambda_3(r_k)$ is real and negative:

$$\lambda_3(r_k) = -d_1(r_k) = -\left(\mu_I + \mu_V + \frac{\gamma \alpha N}{\mu_V} + \frac{r_k \mu_V}{\gamma T_{max} N}\right). \quad (28)$$

Proof. At $r = r_k$, $D(r_k) = 0$, therefore Orlando's formula (26) yields:

$$(\lambda_1(r_k) + \lambda_2(r_k))(\lambda_2(r_k) + \lambda_3(r_k))(\lambda_1(r_k) + \lambda_3(r_k)) = 0. \quad (29)$$

As a consequence of Lemma 3.1, one of the eigenvalues, say $\lambda_3(r_k)$, is negative and λ_1 and λ_2 can not be real non-negative. Therefore $(\lambda_2(r_k) + \lambda_3(r_k))(\lambda_1(r_k) + \lambda_3(r_k))$ can not vanish. It holds that $\lambda_1(r_k) + \lambda_2(r_k) = 0$, hence $\lambda_1(r_k)$ and $\lambda_2(r_k)$ are purely imaginary and conjugate. Let $\lambda_1(r_k) = i\omega_k$, $\lambda_2(r_k) = -i\omega_k$, $\omega_k > 0$ (say).

$$-d_1(r_k) = \lambda_1(r_k) + \lambda_2(r_k) + \lambda_3(r_k) = \lambda_3(r_k),$$

$$d_2(r_k) = \lambda_1(r_k)\lambda_2(r_k) + \lambda_2(r_k)\lambda_3(r_k) + \lambda_3(r_k)\lambda_1(r_k) = \omega_k^2,$$

we can infer that $\lambda_3(r_k) = -d_1(r_k)$ and $\omega_k = \sqrt{d_2(r_k)}$. \square

Theorem 3.3. Under the hypothesis (21), there is a Hopf bifurcation at the critical points $r = r_k$, $k = 1, 2$ (the $(X_i(r_k), r_k)$ are called Hopf points).

Proof. We only need to prove that the derivative of $r \mapsto \lambda_1(r)$ does not vanish at $r = r_k$ (transversality condition). Let us consider the critical point $r = r_1$. From Lemma 3.2 we

know that $\lambda_{1,2}(r_1) = \pm i\omega_1$, $\omega_1 = \sqrt{d_2(r_1)}$. In a neighborhood of r_1 , the mapping $r \mapsto \lambda_1(r)$ is smooth. We compute, differentiating (24):

$$\frac{d\lambda_1}{dr}(r) = -\frac{\lambda_1^2(r)d_1'(r) + \lambda_1(r)d_2'(r) + d_3'(r)}{3\lambda_1^2(r) + 2d_1(r)\lambda_1(r) + d_2(r)}.$$

At $r = r_1$, it comes

$$\frac{d\lambda_1}{dr}(r_1) = -\frac{-d_2(r_1)d_1'(r_1) + i\sqrt{d_2(r_1)}d_2'(r_1) + d_3'(r_1)}{-2d_2(r_1) + 2d_1(r_1)i\sqrt{d_2(r_1)}},$$

hence:

$$\begin{aligned} \frac{d}{dr}(\operatorname{Re} \lambda_1)(r_1) &= \frac{-d_2(r_1)d_1'(r_1) + d_3'(r_1) - d_1(r_1)d_2'(r_1)}{2d_2(r_1) + 2d_1^2(r_1)} \\ &= \frac{1}{\gamma^2 N^2 T_{max}^2 (2d_2 + 2d_1^2)} \left\{ \mu_I \mu_V \gamma^2 N^2 T_{max}^2 \right. \\ &\quad \left. - N\gamma T_{max} (2\gamma N \alpha \mu_V + 2\gamma N \alpha \mu_I + \mu_V^3 + 3\mu_V^2 \mu_I + \mu_V \mu_I^2) \right. \\ &\quad \left. - 2r_1 \mu_I \mu_V^2 - 2r_1 \mu_V^3 \right\}. \end{aligned} \quad (30)$$

Under the hypothesis (21), T_{max} is large, the other quantities including N being fixed. Then the sign of $(d/dr)(\operatorname{Re} \lambda_1)(r_1)$ is clearly positive. On the other hand, $\operatorname{Im} \lambda_1(r_1) = \omega_1 = \sqrt{d_2} > 0$, and $\operatorname{Re} \lambda_3(r_1) = -\operatorname{Re} d_1(r_1) < 0$. According to the classical Hopf bifurcation theorem, there exists a Hopf bifurcation at the critical point $r = r_1$.

A similar argument holds at the other critical point $r = r_2$ at which $(d/dr)(\operatorname{Re} \lambda_1)(r_2) < 0$. \square

3.3. Instability. While the Routh-Hurwitz criterion ensures asymptotic stability, instability does not hold automatically when the criterion is not satisfied. Additional information is needed. We are now in position to complete the analysis.

Theorem 3.4. *Under the hypothesis (21), the infected equilibrium $X_i(r)$ is unstable whenever $r_1 < r < r_2$.*

Proof. Let $N > N_2$ and $r \in (r_1(N), r_2(N))$ be fixed. We have $D_2(r) < 0$. According to Lemma 3.1, $\lambda_3(r) < 0$, say. Hence, by the reciprocal of Ruth-Hurwitz criterion, one of the eigenvalues $\lambda_j(r)$, $j = 1, 2$ has a non-negative real part. Since no one can be real non-negative, it follows that $\lambda_1(r)$ and $\lambda_2(r)$ are complex conjugate. If $\operatorname{Re} \lambda_1$ is positive, instability is proved. Therefore, assume $\operatorname{Re} \lambda_1 = 0$ which implies $\lambda_1(r) + \lambda_2(r) = 0$. Then, by Orlando's formula (26), $D_2(r) = 0$ and we reach a contradiction. More precisely, we have that $\lambda_3(r) < 0$ and $\lambda_1(r)$ and $\lambda_2(r)$ are complex conjugate with positive real part. \square

4. Nonlinear analysis. The framework is the same as in Section 3: $N > 0$ is fixed, T_{max} is large as in (21). Sharper hypotheses will be made below.

Our aim is to study the system (22) in some neighborhood of the critical points r_1 and r_2 , at which Hopf bifurcations occur.

4.1. A local study near the critical values. For r in some neighborhood of r_k , $k = 1, 2$, we subtract the infected equilibria and set $\tilde{X} = X - X_i(r)$, namely $\tilde{X}_1 = T - T_i$, $\tilde{X}_2 = I - I_i$, $\tilde{X}_3 = V - V_i$.

The system (22) now reads for \tilde{X} :

$$\frac{d\tilde{X}}{dt} = J(X_i(r))\tilde{X} + \tilde{\mathcal{F}}(\tilde{X}), \quad (31)$$

where $J(X_i(r))$ is given by (23) and

$$\tilde{\mathcal{F}}(\tilde{X}) = \left(-\frac{r}{T_{max}}\tilde{X}_1^2 - \gamma\tilde{X}_1\tilde{X}_3, \gamma\tilde{X}_1\tilde{X}_3, 0\right).$$

Let us recall that the Jacobian matrix $J(X_i(r))$ has the eigenvalues $\lambda_{1,2}(r_k) = \pm i\omega_k$ and $\lambda_3(r_k) = -d_1(r_k)$, at the critical point $r = r_k$. The corresponding eigenvectors are denoted by $v(r_k)$, $\bar{v}(r_k)$ and $u_3(r_k)$. We set $u_1(k) = \operatorname{Re} v(r_k)$, $u_2(r_k) = \operatorname{Im} v(r_k)$. It comes:

$$u_1 = \begin{pmatrix} \frac{\mu_V s_k}{N(s_k^2 + \omega_k^2)} \\ \frac{\mu_V}{N\mu_I} \\ 1 \end{pmatrix}, \quad u_2 = \begin{pmatrix} \frac{\mu_V \omega_k}{N(s_k^2 + \omega_k^2)} \\ \frac{\omega_k}{N\mu_I} \\ 0 \end{pmatrix}, \quad u_3 = \begin{pmatrix} \frac{\mu_V}{N(\mu_I + \mu_V)} \\ -\frac{1}{N} - \frac{\alpha\gamma}{\mu_V \mu_I} - \frac{r_k \mu_V}{\mu_I \gamma N^2 T_{max}} \\ 1 \end{pmatrix},$$

where $s_k = -\frac{r_k \mu_V}{\gamma T_{max} N} - \frac{\gamma N \alpha}{\mu_V}$.

We define the matrix $P_k = (u_1(r_k), -u_2(r_k), u_3(r_k))$. As P_k is clearly invertible, we set $Q_k = (P_k)^{-1}$. Omitting the subscript k , the coefficients of P_k and Q_k will be respectively denoted by $P_{i,j}$ and $Q_{i,j}$. Under the linear transformation

$$\tilde{X} = PY,$$

the system (31) has the canonical form:

$$\frac{d}{dt} \begin{pmatrix} Y_1 \\ Y_2 \\ Y_3 \end{pmatrix} = \begin{pmatrix} 0 & -\omega_k & 0 \\ \omega_k & 0 & 0 \\ 0 & 0 & -d_1(r_k) \end{pmatrix} \begin{pmatrix} Y_1 \\ Y_2 \\ Y_3 \end{pmatrix} + \begin{pmatrix} F_1 \\ F_2 \\ F_3 \end{pmatrix}, \quad (32)$$

where

$$F = Q_k \tilde{\mathcal{F}}(PY).$$

We also set

$$r = r_k + \mu^k.$$

According to the Hopf bifurcation theorem (see [15, Thms. I and II]), it follows from Theorem 3.3 that, for $k = 1, 2$, the system (32) has, in some neighborhood of $Y = 0$, $\mu^k = 0$, a family of smooth periodic solutions $(Y_{\#}^k(t), \mu^k)$ of period T^k , smoothly parameterized by ε :

$$(Y_{\#}^k(\varepsilon), T^k(\varepsilon), \mu^k(\varepsilon)), \quad \varepsilon \in (0, \varepsilon_0^k), \quad (33)$$

Obviously, ε_0^k depends on all the parameters, especially N and T_{max} . The sign of $\mu^k(\varepsilon)$ determines the direction of the bifurcation, in other words if it is supercritical or subcritical. Another important information is given by the Floquet exponents $\beta^k(\varepsilon)$: the periodic solution is orbitally asymptotically stable with asymptotic phase if $\beta^k(\varepsilon) < 0$, unstable otherwise.

Since the nonlinearities are analytic, μ^k, T^k, β^k are also analytic and have expansions, for $k = 1, 2$, $0 < \varepsilon < \varepsilon_0^k$:

$$\mu^k(\varepsilon) = \mu_2^k \varepsilon^2 + \dots, \quad T^k(\varepsilon) = \frac{2\pi}{\omega_k} (1 + \tau_2^k \varepsilon^2 + \dots), \quad \beta^k(\varepsilon) = \beta_2^k \varepsilon^2 + \dots$$

If the leading terms μ_2^k and β_2^k do not vanish, they provide us with the direction of bifurcation and the stability, respectively.

4.2. Computation of the first Lyapunov coefficient. In order to analyze the bifurcation, we compute the first Lyapunov coefficient $l_1(r_k)$ of the restricted system on the center manifold at the critical parameter values r_k . Loosely speaking, the latter two-dimensional system in the complex variable z reads (see [15, p. 59]),

$$\frac{dz}{dt} = \lambda_1(\mu^k)z + g(z, \bar{z}; \mu^k), \quad (34)$$

where $g(z, \bar{z}; \mu^k)$ is smooth and has a Taylor expansion with coefficients $g_{i,j}(\mu^k)$. The main issue is to control the cubic term in the expansion of (34), namely the sign of the first Lyapunov coefficient (see [21, Sec. 3.4 and 5.4]), which should not vanish (nondegeneracy condition).

To compute the $g_{i,j}(0)$'s, we follow the Recipe-Summary of [15, p. 88-90]. At $Y = 0, \mu^k = 0$:

$$\begin{aligned} g_{11} &= \frac{1}{4} \left(\frac{\partial^2 F_1}{\partial Y_1^2} + \frac{\partial^2 F_1}{\partial Y_2^2} + i \left(\frac{\partial^2 F_2}{\partial Y_1^2} + \frac{\partial^2 F_2}{\partial Y_2^2} \right) \right) \\ &= -\frac{r_k}{2T_{max}} Q_{11}(P_{11}^2 + P_{12}^2) + \frac{1}{2} \gamma P_{11}(Q_{12} - Q_{11}) \\ &\quad + i \left\{ -\frac{r_k}{2T_{max}} Q_{21}(P_{11}^2 + P_{12}^2) + \frac{1}{2} \gamma P_{11}(Q_{22} - Q_{21}) \right\}, \\ g_{02} &= \frac{1}{4} \left(\frac{\partial^2 F_1}{\partial Y_1^2} - \frac{\partial^2 F_1}{\partial Y_2^2} - 2 \frac{\partial^2 F_2}{\partial Y_1 \partial Y_2} + i \left(\frac{\partial^2 F_2}{\partial Y_1^2} - \frac{\partial^2 F_2}{\partial Y_2^2} + 2 \frac{\partial^2 F_1}{\partial Y_1 \partial Y_2} \right) \right) \\ &= \frac{1}{2} \left\{ \frac{r_k}{T_{max}} (Q_{11}(P_{12}^2 - P_{11}^2) + 2Q_{21}P_{11}P_{12}) + \gamma P_{11}(Q_{12} - Q_{11}) \right. \\ &\quad \left. - \gamma P_{12}(Q_{22} - Q_{21}) + i \left[\frac{r_k}{T_{max}} (Q_{21}(P_{12}^2 - P_{11}^2) - 2Q_{11}P_{11}P_{12}) \right. \right. \\ &\quad \left. \left. + \gamma P_{11}(Q_{22} - Q_{21}) + \gamma P_{12}(Q_{12} - Q_{11}) \right] \right\}, \\ g_{20} &= \frac{1}{4} \left(\frac{\partial^2 F_1}{\partial Y_1^2} - \frac{\partial^2 F_1}{\partial Y_2^2} + 2 \frac{\partial^2 F_2}{\partial Y_1 \partial Y_2} + i \left(\frac{\partial^2 F_2}{\partial Y_1^2} - \frac{\partial^2 F_2}{\partial Y_2^2} - 2 \frac{\partial^2 F_1}{\partial Y_1 \partial Y_2} \right) \right) \\ &= \frac{1}{2} \left\{ \frac{r_k}{T_{max}} (Q_{11}(P_{12}^2 - P_{11}^2) - 2Q_{21}P_{11}P_{12}) + \gamma P_{11}(Q_{12} - Q_{11}) \right. \\ &\quad \left. + \gamma P_{12}(Q_{22} - Q_{21}) + i \left[\frac{r_k}{T_{max}} (Q_{21}(P_{12}^2 - P_{11}^2) + 2Q_{11}P_{11}P_{12}) \right. \right. \\ &\quad \left. \left. + \gamma P_{11}(Q_{22} - Q_{21}) - \gamma P_{12}(Q_{12} - Q_{11}) \right] \right\}, \\ G_{21} &= \frac{1}{8} \left(\frac{\partial^3 F_1}{\partial Y_1^3} + \frac{\partial^3 F_1}{\partial Y_1 \partial Y_2^2} + \frac{\partial^3 F_2}{\partial Y_1^2 \partial Y_2} + \frac{\partial^3 F_2}{\partial Y_2^3} \right. \\ &\quad \left. + i \left(\frac{\partial^3 F_2}{\partial Y_1^3} + \frac{\partial^3 F_2}{\partial Y_1 \partial Y_2^2} - \frac{\partial^3 F_1}{\partial Y_1^2 \partial Y_2} - \frac{\partial^3 F_1}{\partial Y_2^3} \right) \right) = 0. \end{aligned}$$

Since the system (32) is three-dimensional, additional computations are needed:

$$\begin{aligned} h_{11} &= \frac{1}{4} \left(\frac{\partial^2 F_3}{\partial Y_1^2} + \frac{\partial^2 F_3}{\partial Y_2^2} \right) \\ &= \frac{1}{2} \left[-\frac{r_k}{T_{max}} Q_{31} (P_{11}^2 + P_{12}^2) + \gamma P_{11} (Q_{32} - Q_{31}) \right], \\ h_{20} &= \frac{1}{4} \left(\frac{\partial^2 F_3}{\partial Y_1^2} - \frac{\partial^2 F_3}{\partial Y_2^2} - 2i \frac{\partial^2 F_3}{\partial Y_1 \partial Y_2} \right) \\ &= \frac{1}{2} \left\{ \frac{r_k}{T_{max}} Q_{31} (P_{12}^2 - P_{11}^2) + \gamma P_{11} (Q_{32} - Q_{31}) \right. \\ &\quad \left. + i \left[\frac{2r}{T_{max}} Q_{31} P_{11} P_{12} - \gamma P_{12} (Q_{32} - Q_{31}) \right] \right\}. \end{aligned}$$

Solving the linear system

$$-d_1 w_{11} = -h_{11}, \quad (-d_1 - 2i\omega_1) w_{20} = -h_{20},$$

we get:

$$w_{11} = \frac{h_{11}}{d_1}, \quad w_{20} = \frac{h_{20}}{d_1 + 2i\sqrt{d_2}}.$$

Furthermore we compute:

$$\begin{aligned} G_{110} &= \frac{1}{2} \left(\frac{\partial^2 F_1}{\partial Y_1 \partial Y_3} + \frac{\partial^2 F_2}{\partial Y_2 \partial Y_3} + i \left(\frac{\partial^2 F_2}{\partial Y_1 \partial Y_3} - \frac{\partial^2 F_1}{\partial Y_2 \partial Y_3} \right) \right) \\ &= \frac{1}{2} \left\{ -\frac{2r_k}{T_{max}} P_{13} (Q_{11} P_{11} + Q_{21} P_{12}) + \gamma (Q_{12} - Q_{11}) (P_{11} + P_{13}) \right. \\ &\quad \left. + \gamma P_{12} (Q_{22} - Q_{21}) + i \left[\frac{2r}{T_{max}} P_{13} (Q_{11} P_{12} - Q_{21} P_{11}) \right. \right. \\ &\quad \left. \left. + \gamma (Q_{22} - Q_{21}) (P_{11} + P_{13}) - \gamma P_{12} (Q_{12} - Q_{11}) \right] \right\}, \\ G_{101} &= \frac{1}{2} \left(\frac{\partial^2 F_1}{\partial Y_1 \partial Y_3} - \frac{\partial^2 F_2}{\partial Y_2 \partial Y_3} + i \left(\frac{\partial^2 F_2}{\partial Y_1 \partial Y_3} + \frac{\partial^2 F_1}{\partial Y_2 \partial Y_3} \right) \right) \\ &= \frac{1}{2} \left\{ \frac{2r_k}{T_{max}} P_{13} (Q_{21} P_{12} - Q_{11} P_{11}) + \gamma (Q_{12} - Q_{11}) (P_{11} + P_{13}) \right. \\ &\quad \left. - \gamma P_{12} (Q_{22} - Q_{21}) + i \left[\frac{2r}{T_{max}} P_{13} (Q_{11} P_{12} + Q_{21} P_{11}) \right. \right. \\ &\quad \left. \left. + \gamma (Q_{22} - Q_{21}) (P_{11} + P_{13}) + \gamma P_{12} (Q_{12} - Q_{11}) \right] \right\}. \end{aligned}$$

Eventually we get:

$$g_{21} = G_{21} + 2G_{110}w_{11} + G_{101}w_{20}.$$

Let us denote $(d\lambda_1/dr)(r_k)$ by $\lambda'_1(r_k)$ which do not vanish, see Thm. 3.3. According to [15, p. 90][21, p. 98-99 and 178], it holds:

Lemma 4.1. For $k = 1, 2$, let

$$c_1(r_k) = \frac{i}{2\omega_k}(g_{20}g_{11} - 2|g_{11}|^2 - \frac{1}{3}|g_{02}|^2) + \frac{g_{21}}{2}. \quad (35)$$

then the first Lyapunov coefficient at r_k reads:

$$l_1(r_k) = \frac{\operatorname{Re} c_1(r_k)}{\omega_k} = \frac{1}{2\omega_k^2} \operatorname{Re}(i g_{20}g_{11} + \omega_k g_{21}), \quad (36)$$

and

$$\mu_2^k = -\frac{\omega_k l_1(r_k)}{\operatorname{Re} \lambda_1'(r_k)}, \quad \beta_2^k = 2\omega_k l_1(r_k). \quad (37)$$

An explicit computation of the $l_1(r_k)$'s is uneasy. We are going to evaluate their sign via an asymptotic method, as well as the signs of μ_2^k and β_2^k .

4.3. Asymptotic analysis. In this part we will take advantage of the limit $T_{max} \rightarrow +\infty$. Passing formally to the limit in (1)-(3), we get to the system

$$\frac{dT}{dt} = \alpha + (r - \mu_T)T - \gamma VT, \quad (38)$$

(2)(3) for $(T^\infty, I^\infty, V^\infty)$, with bifurcation parameter $r - \mu_T$. The latter is nothing but the net T-cell proliferation rate, which changes sign at $r = \mu_T$.

The system (38)(2)(3) is interesting didactically since quite simpler than the original system (1)-(3). However, it has clearly no biological meaning since it would implicate a dysfunction of the homeostatic system. With the same notations and arguments as above, it is not difficult to compute the equilibria X_u^∞ and X_i^∞ and check that

$$N_{crit}^\infty = \frac{\mu_V(\mu_T - r)^+}{\alpha\gamma}.$$

Beside, a Hopf bifurcation occurs at the curve

$$r_1^\infty(N) = \frac{1}{\mu_I \mu_V^3} \left\{ \gamma^2 N^2 \alpha^2 (\mu_I + \mu_V) + \gamma N \alpha \mu_V (\mu_V^2 + \mu_I \mu_V + \mu_I^2) + \mu_V^3 \mu_I \mu_T \right\},$$

with

$$\omega_1^\infty = \sqrt{\frac{\gamma N \alpha \mu_I}{\mu_V} + \gamma \alpha N}.$$

The infected equilibrium X_i^∞ is unstable for $r > r_1^\infty(N)$, the latter region corresponding to (\mathcal{P}^∞) .

Taking the limit $T_{max} \rightarrow +\infty$ in (19), elementary calculations provide the asymptotic behaviors of r_k and ω_k :

Lemma 4.2. Let $N > 0$ be fixed. As $T_{max} \rightarrow +\infty$, it holds:

(i)

$$r_1 = r_1^\infty + O\left(\frac{1}{T_{max}}\right), \quad \omega_1 = \omega_1^\infty + O\left(\frac{1}{T_{max}}\right),$$

(ii)

$$r_2 = \frac{N^2 \gamma^2 \mu_I}{\mu_V (\mu_V + \mu_I)} (T_{max})^2 + O(T_{max}),$$

$$\omega_2 = \sqrt{N \gamma \mu_I T_{max}} + O\left(\frac{1}{(T_{max})^{1/2}}\right).$$

Then it follows immediately from (30) that:

$$\begin{aligned} \operatorname{Re} \lambda'_1(r_1) &= \frac{\mu_I \mu_V}{2 \left(\mu_I + \mu_V + \frac{\gamma \alpha N}{\mu_V} \right)^2 + 2 \left(\frac{\gamma N \alpha \mu_I}{\mu_V} + \gamma \alpha N \right)} + o(1), \\ \operatorname{Re} \lambda'_1(r_2) &= -\frac{\mu_V (\mu_I + \mu_V)^2}{2N^2 \gamma^2 \mu_I (T_{\max})^2} + o\left(\frac{1}{(T_{\max})^2}\right). \end{aligned}$$

A natural idea is to plug these asymptotic formulas in Subsection 4.2. Since the computations are technical but straightforward, we are going to skip them.

Lemma 4.3. *Let $N > 0$ be fixed. As $T_{\max} \rightarrow +\infty$, it holds for the first Lyapunov coefficients at r_k , $k = 1, 2$:*

(i)

$$l_1(r_1) = \frac{\gamma^2 \mu_V^2}{8\omega_1^\infty \mathcal{D}(\gamma^2 \alpha^2 N^2 + 3\gamma \alpha N \mu_I \mu_V + 3\gamma \alpha N \mu_V^2 + \mu_V^2 \mu_I^2 + 2\mu_V^3 \mu_I + \mu_V^4)} \mathcal{H} + o(1),$$

(ii)

$$l_1(r_2) = -\frac{3(\mu_I + \mu_V)^3}{8\gamma^{1/2} N^{5/2} (\mu_I)^{5/2} (T_{\max})^{5/2}} + o\left(\frac{1}{(T_{\max})^{5/2}}\right).$$

In Lemma 4.3, \mathcal{D} and \mathcal{H} are respectively given by

$$\begin{aligned} \mathcal{D}(N) &= (\mu_V \mu_I + \mu_V^2 + \gamma \alpha N)^2 (\mu_V^2 \mu_I^2 + 2\mu_V^3 \mu_I + 6\gamma \alpha N \mu_I \mu_V \\ &\quad + \mu_V^4 + 6\gamma \alpha N \mu_V^2 + \gamma^2 \alpha^2 N^2) (\mu_I + \mu_V), \end{aligned}$$

$$\begin{aligned} \mathcal{H}(N) &= 3\alpha^4 \gamma^4 N^4 (\mu_I + \mu_V)^2 - \alpha^3 \gamma^3 N^3 \mu_V (\mu_I + \mu_V) (12\mu_V^2 + 23\mu_V \mu_I + 12\mu_I^2) \\ &\quad - \alpha^2 \gamma^2 N^2 \mu_V^2 (26\mu_V^4 + 71\mu_I \mu_V^3 + 71\mu_I^3 \mu_V + 26\mu_I^4 + 91\mu_I^2 \mu_V^2) \\ &\quad - \alpha \gamma N \mu_V^3 (\mu_I + \mu_V) (12\mu_V^4 + 25\mu_I \mu_V^3 + 34\mu_I^2 \mu_V^2 + 25\mu_I^3 \mu_V + 12\mu_I^4) \\ &\quad - \mu_V^4 (\mu_I + \mu_V)^2 (\mu_I^4 + 5\mu_I^3 \mu_V - \mu_I^2 \mu_V^2 + 5\mu_I \mu_V^3 + \mu_V^4). \end{aligned}$$

Whereas \mathcal{D} is always positive, the sign of \mathcal{H} varies upon N .

Since $\mathcal{H}(0) < 0$, $\lim_{N \rightarrow +\infty} \mathcal{H}(N) = +\infty$, let us define N_* as the (first) positive zero of \mathcal{H} . Therefore $\mathcal{H} < 0$ for $0 \leq N < N_*$. With the values of Table 1, $N_* \simeq 3.9 \times 10^5$ which is far beyond the biological size of N , therefore this hypothesis is reasonable.

It easily follows from (37) and Lemmas 4.2–4.3 that

$$\mu_2^1 = -\frac{\gamma^2 \mathcal{H}}{4\mu_I \mu_V \mathcal{D}} + o(1), \quad \mu_2^2 = -\frac{3\gamma^2 (\mu_I + \mu_V)}{4\mu_I \mu_V} + o(1).$$

Clearly, if T_{\max} is large enough, the signs of all the above quantities are given by their respective leading terms. More precisely, it holds:

Lemma 4.4. *Let N be fixed, $0 < N < N_*$ (hence $\mathcal{H} < 0$). There exists a $T_{\max}^2 \geq T_{\max}^1$ (see (21)), which depends of $\mu_T, \mu_I, \mu_V, \alpha, \gamma$ and N , such that, whenever $T_{\max} \geq T_{\max}^2$, we have:*

$$\operatorname{Re} \lambda'_1(r_1) > 0, \quad \operatorname{Re} \lambda'_1(r_2) < 0, \quad (39)$$

$$l_1(r_1) < 0, \quad l_1(r_2) < 0, \quad (40)$$

$$\mu_2^1 > 0, \quad \mu_2^2 < 0, \quad \beta_2^1 < 0, \quad \beta_2^2 < 0. \quad (41)$$

We summarize our results in the following Theorem and Corollary which follow from Lemma 4.4 and [15, Thms. I and II]:

Theorem 4.5. *Let N be fixed, $0 < N < N_*$ (hence $\mathcal{H} < 0$). Then, for $k = 1, 2$, for all $T_{max} \geq T_{max}^2$ (given by Lemma 4.4), there exists an $\varepsilon_0^k > 0$ such that the system (32) has a smooth family of nontrivial periodic solutions $(Y_{\#}^k(\varepsilon), \mu^k(\varepsilon))$ with period $T^k(\varepsilon)$, parameterized by $\varepsilon \in (0, \varepsilon_0^k)$. Moreover,*

(i) *as $\varepsilon \rightarrow 0$, $T^k(\varepsilon) \rightarrow 2\pi/\omega_k$ (see (27));*

(ii) *the bifurcation at $\mu^1 = 0$ is supercritical and the periodic solution $Y_{\#}^1(\varepsilon)$ is asymptotically stable with asymptotic phase;*

(iii) *the bifurcation at $\mu^2 = 0$ is subcritical and the periodic solution $Y_{\#}^2(\varepsilon)$ is orbitally asymptotically stable with asymptotic phase.*

It follows from Theorem 4.5:

Corollary 1. *Let N be fixed, $0 < N < N_*$. Then, for $k = 1, 2$, for all $T_{max} \geq T_{max}^2$, there exists an $\varepsilon_0^k > 0$ such that the system (4) has a smooth family of nonconstant periodic solutions $(X_{\#}^k(\varepsilon), r^k(\varepsilon))$ associated with the Hopf points $(X_i(r_k), r_k)$, with period $T^k(\varepsilon)$, and parameterized by $\varepsilon \in (0, \varepsilon_0^k)$:*

$$X_{\#}^k(\varepsilon) = X_i(r_k) + P_k Y_{\#}^k(\varepsilon), \quad r^k(\varepsilon) = r_k + \mu^k(\varepsilon). \quad (42)$$

Moreover,

(i) *as $\varepsilon \rightarrow 0$, $T^k(\varepsilon) \rightarrow 2\pi/\omega_k$ (see (27));*

(ii) *the bifurcation at $r = r_1$ is supercritical and the periodic solution $X_{\#}^1(\varepsilon)$ is asymptotically stable with asymptotic phase;*

(iii) *the bifurcation at $r = r_2$ is subcritical and the periodic solution $X_{\#}^2(\varepsilon)$ is orbitally asymptotically stable with asymptotic phase.*

According to [24, p. 426-427], the number $2\pi/\omega_k$ is called the “virtual period” of the Hopf point $(X_i(r_k), r_k)$.

4.4. “Snake” of orbits. Hereafter we call a nonconstant periodic solution $(X_{\#}(r), r)$ of (1)-(3) an orbit in the (X, r) -space. We have already proved the existence of two families of such orbits $(X_{\#}^k(\varepsilon), r^k(\varepsilon))$, locally near the Hopf point $(X_i(r_k), r_k)$.

The next issue is to investigate whether there exists a “bridge” or “global connection” between the two Hopf points, by a family of orbits. The answer is positive thanks to the theory of “snakes” developed by Mallet-Paret and York [24] (see also [11, p. 27-34]).

According to [24], the Hopf points $(X_i(r_k), r_k)$ are isolated centers. At such an isolated center, the crossing number χ is the net number of pairs of eigenvalues crossing the imaginary axis (see [24, p. 427]). Let $E(r)$ denote the sum of the multiplicities of the eigenvalues of the Jacobian matrix $J(X_i(r))$ having strictly positive real part, then

$$\chi(r_k) = \frac{1}{2}(E(r_{k+}) - E(r_{k-})).$$

Clearly $\chi(r_k)$ is equal to the sign of $\lambda_1'(r_k)$, see Theorem 3.3, hence $\chi(r_1) = +1$, $\chi(r_2) = -1$. Next, the center index is denoted by the Chinese character “中” (*zhong*):

$$\text{中}(X_i(r_k), r_k) = \chi(r_k) (-1)^{E(r_k)}.$$

An isolated center is called a source if $\text{中} = +1$, a sink if $\text{中} = -1$ (see [24, p. 428]). Here we have:

Lemma 4.6. *$\text{中}(X_i(r_1), r_1) = +1$, $\text{中}(X_i(r_2), r_2) = -1$, hence the Hopf points $(X_i(r_1), r_1)$ and $(X_i(r_2), r_2)$ are respectively a source and a sink.*

In the terminology of [24, p. 436], a “snake” is defined in the following way: let $\gamma(\varepsilon)$ be a path (see [24, p. 432]) with domain J and let $Orb(\gamma)$ be the set of orbits $(X_{\#}^k(\varepsilon), r(\varepsilon))$ for which there is an $\varepsilon \in J$ such that $\gamma(\varepsilon)$ is on that orbit. Then, a set of orbits S is called a “snake” if there is maximal oriented path γ such that $Orb(\gamma) = S$.

Theorem 4.7. *There is a unique “snake” S_1 with source (X_i^1, r_1) and sink (X_i^2, r_2) .*

Proof. According to the terminology of [24], the Hopf theorem yields that there is a unique “snake” emanating from a Hopf point. Let us consider the snake S_1 emanating from the source (X_i^1, r_1) , and let us apply the “Snake Termination Principle” (see [24, p. 438-439]). Since S_1 has at least one end, it is an open snake and its sink is either ∞ or a center. From Lemma B.1 (see App. B), it can not be ∞ . The only center which is not (X_i^1, r_1) is (X_i^2, r_2) , which is a sink. Finally, (X_i^1, r_1) is called the source of S_1 , (X_i^2, r_2) its sink. \square

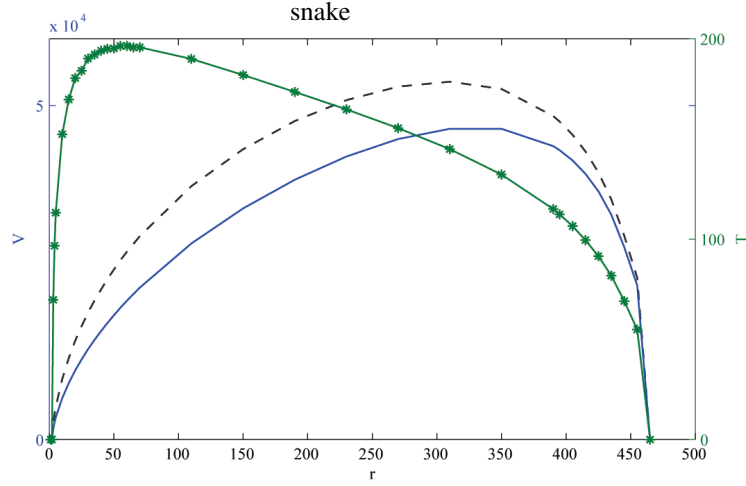


FIGURE 8. Numerical representation of the snake between the source $(X_i(r_1), r_1)$ and the sink $(X_i(r_2), r_2)$. The dotted line represents T , the solid line V and the dashed line $10I$. The variable on the horizontal axis is $r - r_1$, the constant infected equilibrium being normalized to 0.

Remark 2. A further issue is to know whether the elements of S_1 are orbitally asymptotically stable for all values of r , $r_1 < r < r_2$. De Lenheer and Smith [6] observed that the system (1)-(3) gives rise to a three-dimensional competitive dynamical system, in such a case a generalized Poincaré – Bendixson theorem holds in 3D. It follows from [6, Lemma 3.6] and [35, Thm. 1.2] that, for each $r \in (r_1, r_2)$, there is at most a finite number of orbits and at least one is orbitally stable. Unfortunately, we can not infer that the latter belongs to S_1 , although there is a numerical evidence.

5. Numerical results. In view of the numerical computations, we take $N = 300$ to fix ideas. Other parameters are as in Table 1. Initial data are $T_0 = T_u$, $I_0 = 0.0$, $V_0 = 0.0185$.

We start from the value $r_{crit} = 0.05625$; then, we increase the logistical parameter r monotonically, until a critical condition is reached at which any further change would result in instability.

We present the graphs of numerical solution of the system (1)-(3) and the trajectory of the solutions in the T - V - I space, see Figures 9-12. In Figures 10 and 11 corresponding to subdomain (\mathcal{P}) , the solution approaches periodic orbits.

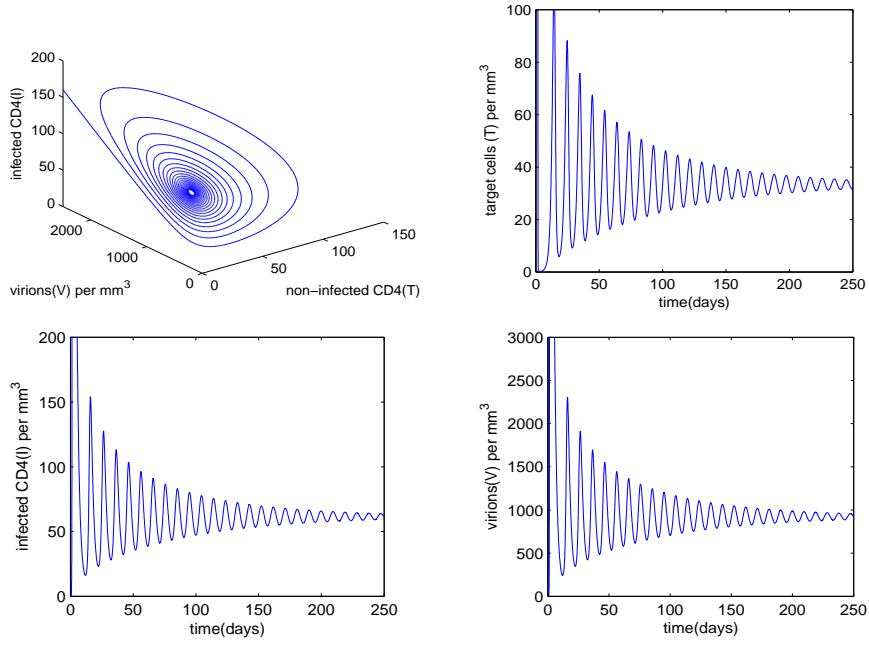


FIGURE 9. Numerical solution of the system (1)-(3) in the domain (\mathcal{I}) . Parameter values are $N = 300$ and $r_{crit} = 0.05625 < r = 1.0 < r_1 = 2.1846$. The infected equilibrium is stable.

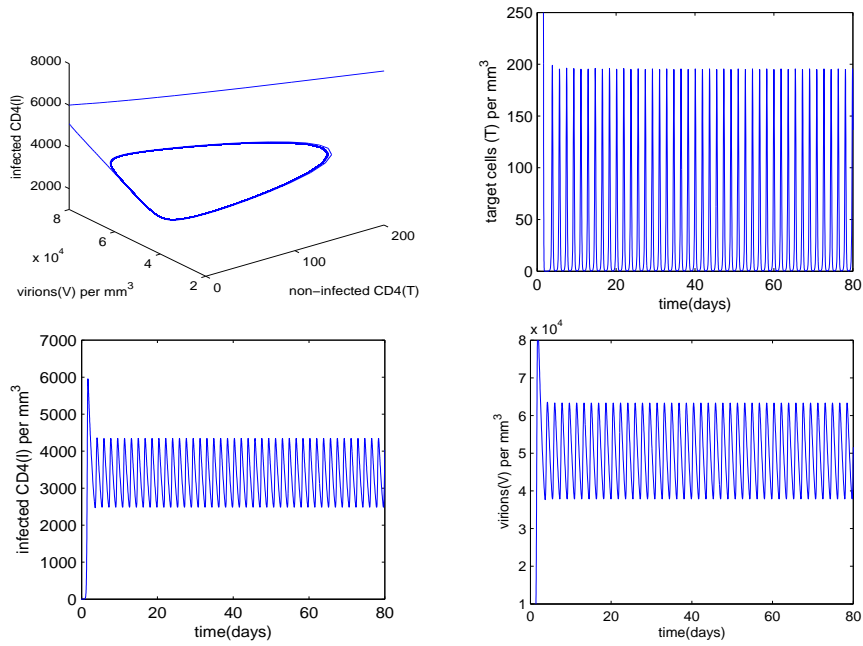


FIGURE 10. Numerical solution of the system (1)-(3) in (\mathcal{P}) . Parameter values are $N = 300$ and $r_1 < r = 50.0 < r_2$. The infected equilibrium is unstable, a periodic orbit is observed.

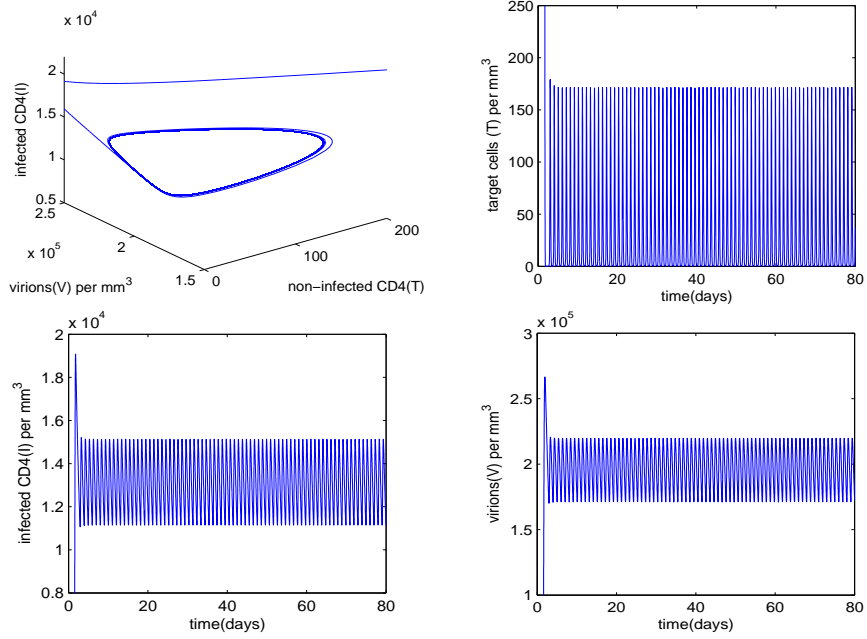


FIGURE 11. Numerical solution of the system (1)-(3) in (\mathcal{P}) . Parameter values are $N = 300$ and $r = 200.0 < r_2 = 464.1225$. The infected equilibrium is unstable, a periodic orbit is observed.

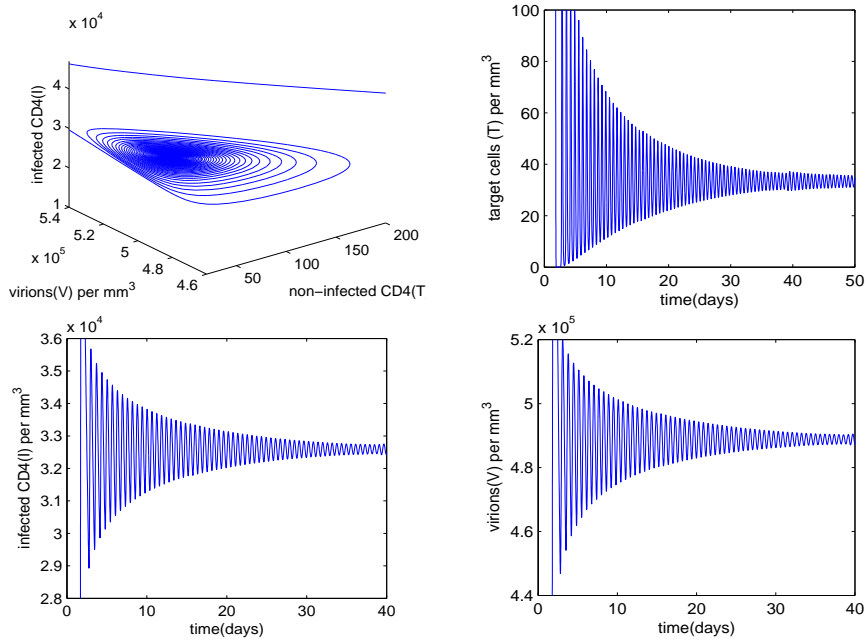


FIGURE 12. Numerical solution of the system (1)-(3) in (\mathcal{I}) . Parameter values are $N = 300$ and $r = 500.0 > r_2 = 464.1225$. The infected equilibrium is again stable.

6. Conclusion. In summary, the infected equilibria are asymptotically stable in a region (\mathcal{I}) , except in an explicit subdomain (\mathcal{P}) which may be biologically interpreted as a perturbation of the infection by a specific or unspecific immune response against HIV. The existence of Hopf bifurcations and periodic orbits in (\mathcal{P}) lead to some very interesting mathematical issues which, as far as we know, have not been fully addressed in previous articles on the logistic HIV model. In a forthcoming paper [10], we will take the viral diffusion into account (see [4]).

Studying the subdomain (\mathcal{P}) in models taking antiretroviral treatment into account and/or studying the impact of immunotherapy may allow generating new hypotheses on HIV elimination.

Appendix A. The “full” logistic model. It is possible to replace (1) by

$$\dot{T} = \alpha - \mu_T T + rT \left(1 - \frac{T+I}{T_{max}}\right) - \gamma VT, \quad (43)$$

(see [5, 31]). However, the proportion of infected cells is very small, on the order of 10^{-4} to 10^{-5} of T cells, therefore this correction in the logistic proliferation term may be ignored (see [31, p. 10]). Wang and Li [34] studied the global dynamics of the system (43)(2)(3). Again, the boundary of (\mathcal{P}) is the locus of points (N, r) such that $D_2(N, r) = 0$, where

$$\begin{aligned} D_2(N, r) = & \frac{1}{\mu_V^2 (T_{max}^2 \gamma^2 N^2 (\mu_V r + \gamma N \mu_I T_{max}))} \left(\mu_V^4 (\mu_V^2 + \mu_I N \gamma T_{max}) r^3 \right. \\ & + \mu_V^2 N \gamma T_{max} (\mu_V^4 + 3\mu_V^3 \mu_I + \mu_V^2 \mu_I^2 - \mu_V^2 \mu_I \mu_T + \mu_V \mu_I^2 N \gamma T_{max} + \alpha N^2 \gamma^2 \mu_I T_{max} \\ & + 2\mu_V \mu_I N \gamma \alpha + 2N \gamma \alpha \mu_V^2) r^2 + \mu_V N^2 \gamma^2 T_{max}^2 (N^2 \gamma^2 \alpha^2 \mu_V + \mu_V^3 N \gamma \alpha \\ & + 4\mu_V \mu_I^2 N \gamma \alpha - \mu_I^2 \mu_V^2 N \gamma T_{max} - \mu_V^2 \mu_I^2 \mu_T + 3\mu_V^3 \mu_I^2 - N \gamma \alpha \mu_I \mu_V \mu_T \\ & + \mu_V^4 \mu_I + 2N^2 \gamma^2 \alpha^2 \mu_I + 4\mu_V^2 N \gamma \mu_I \alpha + \mu_V^2 \mu_I^3) r + \mu_I N^3 \gamma^3 T_{max}^3 (\mu_I \gamma N \mu_V^2 \alpha \\ & \left. + \gamma^2 N^2 \alpha^2 \mu_V + \mu_I^2 \gamma N \mu_V \alpha + \mu_I \gamma^2 N^2 \alpha^2 + \gamma N \mu_V^3 \alpha + \mu_I \mu_V^3 \mu_T) \right). \end{aligned}$$

Numerical evidence (see Fig. 13) shows that the subdomain (\mathcal{P}) is bounded, in contrast to the situation of the model with (1). Moreover, the shape of the boundary of (\mathcal{P}) is reminiscent of an “isola” in bifurcation theory (see [7]).

Finally, as other authors, we omitted the term $-\gamma VT$ in (3), but its omission is as an approximation (see e.g., [30]).

Appendix B. Boundness lemma.

Lemma B.1. *The solution of the system (1)-(3) remains bounded for all times $t > 0$.*

Proof. Let $(T(t), I(t), V(t))$ the solution of the system (1)-(3) with non-negative initial data $(T(0), I(0), V(0))$. It is not difficult to check that the non-negative octant \mathbb{R}^3 is positively invariant with respect to the system.

From (1), we observe that

$$\frac{dT}{dt} \leq \alpha - \mu_T T + rT \left(1 - \frac{T}{T_{max}}\right).$$

Let $\Delta T(t) = T(t) - T_u$:

$$\begin{aligned} \frac{d(\Delta T)}{dt} & \leq \alpha - \mu_T (T_u + \Delta T) + r(T_u + \Delta T) \left(1 - \frac{T_u + \Delta T}{T_{max}}\right) \\ & = (r - \mu_T) \Delta T - \frac{r}{T_{max}} (\Delta T)^2 - \frac{2r \Delta T T_u}{T_{max}}. \end{aligned}$$

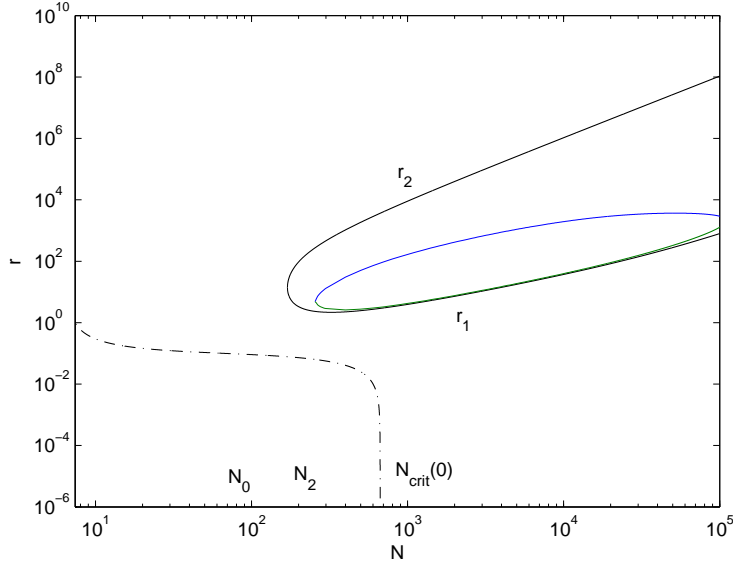


FIGURE 13. Comparison of the “perturbated” subdomains (\mathcal{P}). The closed curve is the “isola” in the “full” logistic model.

By substituting the value of T_u , see (5):

$$\frac{d(\Delta T)}{dt} \leq -\frac{r}{T_{max}}(\Delta T)^2 - s\Delta T \leq -s\Delta T,$$

where $s = \sqrt{(r - \mu_T)^2 + \frac{4\alpha r}{T_{max}}} > 0$. Then, it comes $\frac{d}{dt}(e^{st} \Delta T) \leq 0$, hence $\Delta T(t) \leq e^{-st} \Delta T(0)$. Set $M = \max\{T_u, T(0)\}$, thus

$$T(t) \leq e^{-st} T(0) + (1 - e^{-st}) T_u \leq M,$$

therefore $T(t)$ is bounded.

Next, let us set $L(t) = T(t) + I(t)$. It follows from (1) and (2):

$$\begin{aligned} \frac{dL}{dt} &= \alpha - \mu_T T + rT \left(1 - \frac{T}{T_{max}}\right) - \mu_I I \\ &\leq \alpha - mL + rT_{max} \left(1 - \frac{T}{T_{max}}\right) \frac{T}{T_{max}} \\ &\leq -mL + M_1, \end{aligned}$$

where $m = \min(\mu_T, \mu_I)$ and $M_1 = \alpha + rT_{max}/4$. It yields:

$$L(t) \leq \frac{M_1}{m} + (L(0) - \frac{M_1}{m})e^{-mt},$$

therefore $L(t)$ is bounded, and so is $I(t) = L(t) - T(t)$. Finally, it follows from (3) that $V(t)$ is also bounded. \square

Acknowledgments. We gratefully thank Odo Diekmann and Luca Lorenzi for their comments.

REFERENCES

- [1] R. Antia, V. V. Ganusov and R. Ahmed, *The role of models in understanding CD8+ T-cell memory*, Nat. Rev. Immunol., **5** (2005), 101–111.
- [2] A. Babiker, S. Darby, D. De Angelis, D. Kwart, K. Porter, V. Beral, J. Darbyshire, N. Day, N. Gill, R. Coutinho, and others, *Time from HIV-1 seroconversion to AIDS and death before widespread use of highly-active antiretroviral therapy: a collaborative re-analysis*, Lancet, **355** (2000), 1131–1137.
- [3] J. N. Blankson, D. Persaud and R. F. Siliciano, *The challenge of viral reservoirs in HIV-1 infection*, Annu. Rev. Med., **53** (2002), 557–593.
- [4] C. -M. Brauner, D. Jolly, L. Lorenzi and R. Thiebaut, *Heterogeneous viral environment in a HIV spatial model*, Discrete Cont. Dyn.-B, **15** (2011), 545–572.
- [5] R. V. Culshaw and S. Ruan, *A delay-differential equation model of HIV infection of CD4+ T-cells*, Math. Biosci., **165** (2000), 27–39.
- [6] P. De Leenheer and H. L. Smith, *Virus dynamics: a global analysis*, SIAM J. Appl. Math., **63** (2003), 1313–1327.
- [7] D. Dellwo, H. B. Keller, B. J. Matkowsky and E. L. Reiss, *On the birth of isolas*, SIAM J. Appl. Math., (1982), 956–963.
- [8] O. Diekmann and J. A. P. Heesterbeek, “Mathematical epidemiology of infectious diseases,” Wiley Chichester, 2000.
- [9] D. C. Douek, J. M. Brenchley, M. R. Betts, D. R. Ambrozak, B. J. Hill, Y. Okamoto, J. P. Casazza, J. Kurruppu, K. Kunstman, S. Wolinsky and others, *HIV preferentially infects HIV-specific CD4+ T cells*, Nature, **417** (2002), 95–98.
- [10] X.Y. Fan, C. -M. Brauner and L. Lorenzi, *Two dimensional stability in a HIV model with logistic growth term*, to appear.
- [11] B. Fiedler, “Global bifurcation of periodic solutions with symmetry,” Springer-Verlag (Berlin and New York), 1988.
- [12] D. Finzi, J. Blankson, J. D. Siliciano, J. B. Margolick, K. Chadwick, T. Pierson, K. Smith, J. Lisiewicz, F. Lori, C. Flexner and others, *Latent infection of CD4+ T cells provides a mechanism for lifelong persistence of HIV-1, even in patients on effective combination therapy*, Nat. Med., **5** (1999), 512–517.
- [13] F. R. Gantmakher, “The theory of matrices,” Chelsea Pub Co, 2000.
- [14] P. Hartman, “Ordinary Differential Equations,” Birkhäuser, Boston, 1982.
- [15] B. D. Hassard, N. D. Kazarinoff and Y. H. Wan, “Theory and applications of Hopf bifurcation,” CUP Archive, 1981.
- [16] D. D. Ho, A. U. Neumann, A. S. Perelson, W. Chen, J. M. Leonard, M. Markowitz and others, *Rapid turnover of plasma virions and CD4 lymphocytes in HIV-1 infection*, Nature, **373** (1995), 123–126.
- [17] S. C. Jameson, *Maintaining the norm: T-cell homeostasis*, Nat. Rev. Immunol., **2** (2002), 547–556.
- [18] S. C. Jameson, *T cell homeostasis: keeping useful T cells alive and live T cells useful*, Semin. Immunol., **17** (2005), 231–237.
- [19] L. E. Jones and A. S. Perelson, *Transient viremia, plasma viral load, and reservoir replenishment in HIV-infected patients on antiretroviral therapy*, J. Acquir. Immune. Defic. Syndr., **45** (2007), 483–493.
- [20] T. Katō, “Perturbation theory for linear operators,” 2nd edition, Springer Verlag, 1980.
- [21] Y. A. Kuznetsov, “Elements of applied bifurcation theory,” Springer Verlag, 1998.
- [22] Y. Levy, H. Gahery-Segard, C. Durier, A. S. Lascaux, C. Goujard, V. Meiffredy, C. Rouzioux, R. E. Habib, M. Beumont-Mauviel, J. G. Guillet and others, *Immunological and virological efficacy of a therapeutic immunization combined with interleukin-2 in chronically HIV-1 infected patients*, AIDS, **19** (2005), 279–286.
- [23] Y. Levy, C. Lacabaratz, L. Weiss, J. P. Viard, C. Goujard, J. D. Lelievre, F. Boue, J. M. Molina, C. Rouzioux, V. Avettand-Fenoel and others, *Enhanced T cell recovery in HIV-1-infected adults through IL-7 treatment*, J. Clin. Invest., **119** (2009), 997.
- [24] J. Mallet-Paret and J. A. Yorke, *Snakes: Oriented families of periodic orbits, their sources, sinks, and continuation*, J. Differ. Equations, **43** (1982), 419–450.
- [25] A. J. McMichael, P. Borrow, G. D. Tomaras, N. Goonetilleke and B. F. Haynes, *The immune response during acute HIV-1 infection: clues for vaccine development*, Nat. Rev. Immunol., **10** (2009), 11–23.
- [26] M. A. Nowak and R. M. May, “Virus dynamics,” Oxford University Press, 2000.
- [27] G. Pantaleo, C. Graziosi and A. S. Fauci, *New concepts in the immunopathogenesis of human immunodeficiency virus infection*, N. Engl. J. Med., **328** (1993), 327–335.
- [28] A. S. Perelson, *Modelling viral and immune system dynamics*, Nat. Rev. Immunol., **2** (2002), 28–36.
- [29] A. S. Perelson, P. Essunger, Y. Cao, M. Vesanen, A. Hurley, K. Saksela, M. Markowitz and D. D. Ho, *Decay characteristics of HIV-1-infected compartments during combination therapy*, Nature, **387** (1997), 188–191.

- [30] A. S. Perelson, D. E. Kirschner and R. De Boer, *Dynamics of HIV infection of CD4+ T cells*, Math. Biosci., **114** (1993), 81–125.
- [31] A. S. Perelson and P. W. Nelson, *Mathematical analysis of HIV-I: dynamics in vivo*, SIAM Rev., **41** (1999), 3–44.
- [32] A. S. Perelson, A. U. Neumann, M. Markowitz, J. M. Leonard and D. D. Ho, *HIV-1 dynamics in vivo: virion clearance rate, infected cell life-span, and viral generation time*, Science, **271** (1996), 1582–1586.
- [33] J. D. Siliciano, J. Kajdas, D. Finzi, T. C. Quinn, K. Chadwick, J. B. Margolick, C. Kovacs, S. J. Gange and R. F. Siliciano, *Long-term follow-up studies confirm the stability of the latent reservoir for HIV-1 in resting CD4+ T cells*, Nat. Med., **9** (2003), 727–728.
- [34] L. Wang and M. Y. Li, *Mathematical analysis of the global dynamics of a model for HIV infection of CD4+ T cells*, Math. Biosci., **200** (2006), 44–57.
- [35] H. R. Zhu and H. L. Smith, *Stable periodic orbits for a class of three dimensional competitive systems*, J. Differ. Equations, **110** (1994), 143–156.

Received 19 December 2011; revised 11 May 2012.

E-mail address: fan.xinyue@163.com

E-mail address: cmbrauner@gmail.com

E-mail address: linda.wittkop@isped.u-bordeaux2.fr